JOURNAL OF MATERIALS SCIENCE 37 (2002) 433–460

The toughening of cyanate-ester polymers

Part I *Physical modification using particles, fibres and woven-mats*

A. J. KINLOCH, A. C. TAYLOR
Department of Mechanical Engineering, Imperial College of Science, Technology and Medicine, Exhibition Road, London, SW7 2BX, UK
E-mail: a.kinloch@ic.ac.uk; a.c.taylor@ic.ac.uk

A fracture mechanics approach has been used to investigate the effects of the addition of physical modifiers on the fracture energy, G_c, of brittle cyanate-ester polymers. Tests were performed using adhesive joint specimens at −55, 21 and 150°C, with all the specimens exhibiting cohesive failure in the cyanate-ester adhesive layer. The fracture energies of systems modified using a range of inorganic and thermoplastic particles, fibres and woven-mats have been measured, and scanning electron microscopy has been used to determine the toughening micromechanisms involved. Firstly, it is shown that the addition of 10% by weight of particulate modifiers can increase the fracture energy of the cyanate-ester polymer by 100%, due to a combination of toughening micromechanisms such as crack deflection, pinning and matrix cavitation around the second-phase particles. These experimental data have been compared to predictions from an analytical model. Secondly, it is demonstrated that the use of long fibres or woven-mats can give an a major increase in the value of the fracture energy, G_c, at initiation, and a further increase with increasing crack length, i.e. a significant '*R*-curve' effect is observed. At relatively long crack lengths, the measured fracture energy may be six times greater than that of the unmodified polymer value, due to fibres debonding and bridging across the fracture surfaces. Finally, it is shown that several of the physically-modified polymers developed in the present work have fracture energies that are greater than a typical commercially-available cyanate-ester film adhesive.

1. Introduction

The use of adhesive bonding in industry has increased steadily in recent years, and structural adhesives have replaced mechanical fastening, spot-welding, brazing, etc. methods in many applications. However, the use of adhesives at high temperatures is limited by their relatively low maximum service-temperatures. These result from two main features of the nature of modern structural adhesives. Firstly, most formulations are based upon epoxy polymers, which are unstable and degrade when exposed to relatively high temperatures. Indeed, the maximum glass transition temperatures, T_g, for epoxy polymers lie in the range of 200 to 250°C, while their maximum long-term service temperature will typically be about 175°C [1]. Secondly, most structural adhesives are toughened by the presence of a second, dispersed, rubbery phase and their maximum service temperature is also restricted by the presence of such rubber particles [2]. In order for the maximum service temperature to be significantly increased, a high-temperature resistant resin, such as a cyanate ester, may be used to replace the epoxy resin. However, the second-phase rubber particles also need to be replaced by another material with a better elevated-temperature stability. This replacement material must, of course, also impart a significantly improved toughness to the base resin that is employed, since all the temperature-resistant polymers tend to be very brittle. The typical adhesive performance required for these high-temperature applications is the ability to survive for 20,000 hours in air at 150°C, with a T_g above 250°C.

As mentioned above, the alternatives to epoxy-based resin systems include cyanate-ester resins. Cyanate-ester polymers are known to possess good long-term thermal stability [3] and their glass transition temperatures can be very high, typically around 290°C [4, 5]. The cyanate-ester monomers are esters of bisphenols and cyanic acid, which contain reactive ring-forming -O-C ≡ N groups, see Fig. 1, and cure to form thermoset polymers. During curing, they form three-dimensional networks of oxygen-linked triazine (cyanurate) and bisphenyl units, as shown in Fig. 2 [6, 7]. However, the cured polymers are very brittle, and need to be toughened to make them useful engineering polymers. One method of increasing the toughness is to chemically co-react a phenol with the simple cyanate-ester monomer during the polymerisation reaction. Nevertheless, the incorporation of a phenol into the cyanate-ester

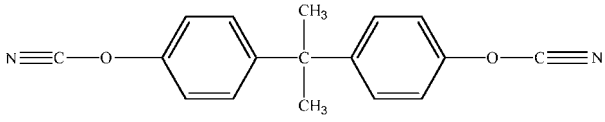

Figure 1 Structural model of the BADCy cyanate-ester monomer [6].

polymer structure only produces a relatively small increase in the toughness, and a significant increase in toughness can only be achieved by the formation of a multiphase structure for the thermoset polymer.

The present paper, Part I, discusses the use of inorganic and thermoplastic particulates, fibres and woven-mats which act to physically modify the base cyanate-ester resins to give a multiphase nano- or micro-structure for the cured polymer. Clearly, the aim is to increase the toughness, but without sacrificing the high-temperature properties, of the formulated polymer. Both the simple cyanate-ester resin and the co-reacted phenol and cyanate-ester resins are employed as the base materials. In the present work, the fracture energies, G_c, of the unmodified and physically-modified cyanate-ester polymers have been measured over a range of test temperatures, from −55 to 150°C. These fracture tests have been conducted using the tapered double-cantilever beam (TDCB) adhesive joint geometry, employing surface-pretreated aluminium-alloy substrates. This test method has the advantages that (a) only small quantities of material are needed to conduct a valid fracture-mechanics test, and (b) the surface pretreatment for the substrates can be selected such that cohesive failure through the adhesive layer occurs, and this avoids the difficulties that arise in the interpretation of the results when interfacial failure results. The effects on the toughness, G_c, of (a) the concentration of the added modifiers, (b) the particle size of the added modifiers, and (c) the test temperature are investigated. These data are used, together with the results from electron microscopy studies, to identify the toughening micromechanisms and the measured fracture energies are compared to values predicted from an analytical toughening model.

In Part 2 of the present work [8] the effects of chemical modification of the cyanate-ester resins are reported. In Part 2, the blending of functionally-active thermoplastic modifiers, such as reactively-terminated poly(ether sulphone), with several different cyanate-ester resins are discussed. The effects of the concentration of the chemical-modifier and the test temperature are investigated, and the relationships between the microstructure of the polymers and the values of the measured toughness are reported. The toughening micromechanisms are also identified and contrasted to those found for the physical modifiers reported in the present paper. Also, in Part 2, the long-term ageing of specimens (using unmodified, physically-modified and chemically-modified cyanate-ester polymers) in air at 150°C, for up to 7500 hours, is discussed.

2. Experimental

2.1. Materials

The substrates used to form the tapered double-cantilever beam (TDCB) joints were aluminium alloy, grade EN-AW-2014A [9]. The cyanate-ester monomer used was 'bisphenol-A dicyanate' (BADCy) supplied by Lonza (Düren, Germany). The monomer was pre-polymerised to 44% conversion of cyanate groups [10] by the Institüt Fraunhofer Zuverlässigkeit und Microintegration (Teltow, Germany) to give the simple cyanate-ester, termed 'BADCy', resin used in the present studies. This was achieved by heating the monomer to 180°C and maintaining it at that temperature until the required conversion was reached. (The degree of conversion was ascertained as described below.)

A range of particulate and fibre modifiers was used, and these are listed in Table I. They were selected to be thermally-stable materials, and clearly the inorganic modifiers listed in Table I achieve this requirement. The polymers shown in Table I were chosen as they are represent some of the most thermally-stable polymeric materials which are available as particulates and/or fibres. These physical modifiers were also chosen to represent a range of particle sizes and shapes, as well as a range of

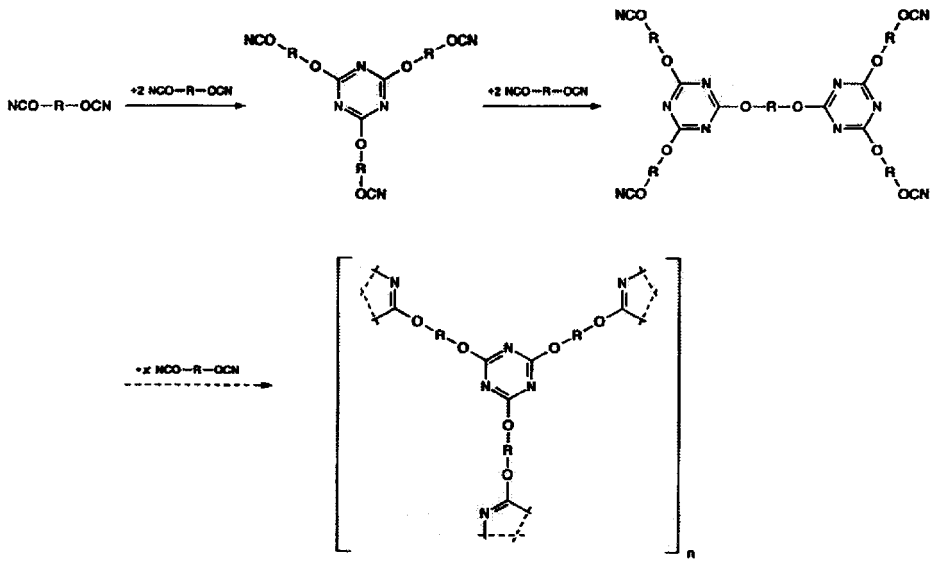

Figure 2 Curing of the simple cyanate-ester resins, from [7].

TABLE I Physical modifiers used in the present work

Modifier	Size	Supplier
Alumina, Al_2O_3	$\sim$0.1 μm	Goodfellow, UK
Alumina, Al_2O_3	$\sim$20 nm	Nanopowder Inc., USA
Carbon short-fibres	7 μm fibre diameter, 1 mm long	Goodfellow, UK
Glass-fibre woven-mat	10 μm fibre diameter, woven mat	Goodfellow, UK
Hollow glass spheres	9–13 μm diameter	Potters-Ballotini, UK
Kevlar short-fibres	1 mm long	DuPont, UK
Muscovite mica	10 μm	Microfine Minerals, SX400, UK
Muscovite mica	40 μm	Microfine Minerals, P66, UK
Muscovite mica	80 μm	Microfine Minerals, R120, UK
PEEK powder	$<$200 μm	Goodfellow, UK
PEEK monofilament	200 μm fibre diameter	Goodfellow, UK
PEEK fibre	34 μm fibre diameter, 30 filaments per tow	Goodfellow, UK
PEEK woven-mat	300 μm monofilament diameter, twill weave	Zyek, UK
PTFE powder	6–9 μm	Goodfellow, UK
Silicon dioxide, SiO_2	$\sim$20 nm	Nanopowder Inc., USA
Titania, TiO_2	$\sim$20 nm	Nanopowder Inc., USA
Wollastonite	10 μm diameter, 50 μm long	Microfine Minerals, UK
Yttrium oxide, Y_2O_3	$\sim$20 nm	Nanopowder Inc., USA

materials, including both the inorganic and polymeric materials. Approximately spherical particles with diameters between 20 nm and 200 μm were used, as well as rod-like wollastonite and plate-like mica particles. Short and long fibres, 1 mm and 300 mm in length respectively, were used, as well as woven mats. The percentages added are based upon weight percents of the simple BADCy resin. Although for the cyanate-ester resins which were chemically-modified with the 4-cumylphenol, see below, the weight percentage of the physical modifier when added was based upon the weight of the phenol co-reacted BADCy resin present.

In addition to the simple BADCy resin, a range of cyanate-ester resins were prepared by co-reacting the BADCy material with 5, 10 and 15 w/w% of 4-cumylphenol [10]. The 4-cumylphenol is monofunctional, so its inclusion will reduce the crosslink density of the network [7] and hence may increase somewhat the fracture energy, G_c, of the unmodified cyanate-ester resin. Finally, for comparison, a commercial cyanate-ester based film adhesive, 'Metlbond 2555G' (Cytec, USA), was also studied.

2.2. Specimen manufacture

Prior to bonding, the two substrates needed to form the TDCB specimen were abraded using 180/220 mesh alumina grit, solvent cleaned in hot trichloroethylene, and etched [11] in chromic-sulphuric acid for 20 minutes at 69°C. The substrates were rinsed with tap water, placed in a bath of tap water for 10 minutes, and rinsed with distilled water. The substrates were then placed in an oven at 140°C for 30 minutes.

In the case of the particulate and short-fibre modifiers, the prepolymerised resin, which was solid at room temperature, was ground into a powder. The physical modifiers were added and mixed thoroughly with the powdered resin. The powdered physical-modifier and resin mixture was placed on the warm substrates, allowed to melt, and then spread over the two substrates using a spatula. In the case of the mats and long fibres, the prepolymerised resin was again first ground into a powder. The powdered resin was placed on the warm substrates, allowed to melt, and spread using a spatula. Next, the mats and long fibres were placed on the molten resin, and tapped into place using a spatula. For both preparation methods, wire shims, 0.25 mm in diameter, were placed at either end of the substrates to control the thickness of the cyanate-ester adhesive layer. A piece of release-coated aluminium foil was placed on each substrate, extending 80 mm from the loading point, to act as a starter crack. The joints were cured for 16 hours at 180°C, 4 hours at 220°C followed by 1 hour at 260°C, and allowed to cool slowly in the oven. However, the final, maximum, cure temperature used was reduced to 240°C for the cyanate-ester resin with 10 w/w% co-reacted phenol, and to 220°C with the 15 w/w% co-reacted phenol.

For the specimens made using the 'Metlbond 2555G' adhesive, the substrates were surface pretreated as described above. The cyanate-ester film adhesive, which was sandwiched between two protective backing films, was cut using a scalpel to be a few millimetres wider than the TDCB substrate. One piece of backing film was removed, and the adhesive applied to one substrate. The other piece of backing film was removed, and an aluminium starter foil was placed in position. (Wires were not used in these joints to control the bondline thickness.) The joints were cured for 4 hours at 180°C, followed by 2 hours at 230°C, and then allowed to cool slowly in the oven.

2.3. Fracture testing

Fracture testing of the TDCB joints was performed at a constant displacement rate of 0.1 mm/min, according to the method described in the draft ESIS (European Structural Integrity Society) protocol [12, 13]. These fracture tests were performed at -55, 21 and 150°C. Prior to testing, the length of the aluminium starter foil was measured, and any excess adhesive was removed from the side of the specimens. One side of each specimen was spray-painted with a thin layer of white paint, and a paper scale, marked every 1 mm, was adhered to the side of the substrate above the adhesive layer.

The specimens were loaded at a constant displacement rate of 0.1 mm/min until a crack was seen to propagate from the starter foil, when they were unloaded

back to zero load at 0.5 mm/min. This precracking stage ensures that there is a sharp precrack present in the specimen prior to the actual test. The specimens were loaded again at 0.1 mm/min, and the crack propagation was followed using a travelling microscope. Once about 100 mm of crack propagation had been observed, the specimens were unloaded at 0.5 mm/min. The specimens were then broken open at 5 mm/min.

Force, displacement and crack length data were recorded. These data were analysed to provide values of the fracture energy. Straight lines were fitted to the loading and unloading lines of the force versus displacement response, and the difference in displacement between the displacement axis intercepts was calculated. This offset displacement was divided by the maximum displacement. If the resultant fraction was less than 0.05, then it was assumed that no plastic deformation of the substrates occurred [13]. In the present work, the resultant fraction was always less than 0.05 and, indeed, no plastic deformation of the substrate arms of the TDCB specimens was ever visually observed.

The TDCB specimen geometry has been used extensively to measure the fracture energy, G_c, of adhesives [14–16]. The TDCB substrates were tapered to give a linear change in compliance, C, with crack length, a. The beams were 310 mm long, 10 mm wide, and the height, z, was defined by a constant, m_b, such that $m_b = 2\ mm^{-1}$, where m_b is given by:

$$m_b = \left(\frac{3a^2}{z^3} + \frac{1}{z}\right) \quad (1)$$

The values of the fracture energy, G_c, were calculated using a linear-elastic fracture-mechanics method. The simple beam theory approach was used [13], which yields:

$$G_c = \frac{4P_c^2 m_b}{E_s B^2} \quad (2)$$

where G_c is the adhesive fracture energy, P_c is the failure load, E_s is the substrate modulus, and B is the specimen width. The value of m_b equals 2 mm^{-1}.

The crack always grew cohesively through the adhesive layer and several types of crack growth were observed:

(a) Stable crack growth accompanied by no 'R-curve'. An 'R-curve' is where the toughness, i.e. the material's resistance to fracture, increases as the crack grows. However, here the crack grew in a steady manner and the value of the fracture energy, G_c, was independent of the length of the propagating crack.

(b) Stable crack growth accompanied by an 'R-curve'. Here the crack grew in a steady manner but the value of the fracture energy, G_c, increased as the crack propagated through the specimen. In the illustrated results, the minimum value (i.e. the initiation value at short crack lengths) and the maximum value (i.e. at relatively long crack lengths) of G_c are both quoted.

(c) Stick/slip crack growth, where the crack initiated and then propagated in a rapid, unstable manner through the specimen until it arrested. Thus, the measured load versus displacement trace has the characteristic 'sawtooth' appearance. Values of G_c associated with crack initiation and crack arrest may therefore be deduced. When failure was in a stick/slip manner, the values of the fracture energy quoted were calculated from the load associated with crack initiation, rather than with crack arrest.

(d) In a few instances, failure occurred in a partially stable and a partially stick/slip manner. In such cases, the value of the fracture energy, G_c, for stable crack propagation is quoted.

The coefficients of variation for the values of the fracture energy, G_c, so ascertained were typically ±8%.

3. Results and discussion: simple BADCy polymer

3.1. Introduction

The results from the fracture tests will be discussed for each formulation. Firstly, the simple BADCy resin will be considered and the effects of modifying it with the particulate, short-fibre, long-fibre and woven-mat materials will be considered. Secondly, base resins which consist of this BADCy monomer co-reacted with various concentrations of the 4-cumylphenol will be discussed in Section 4, together with the effects of the addition of various physical modifiers. Finally, these data will be compared in Section 5 to the results for a commercially-available cyanate-ester system, i.e. the 'Metlbond 2555G' adhesive.

3.2. Unmodified BADCy polymer

To determine the extent of cure of the unmodified, simple cyanate-ester resin, Fourier transform infrared spectroscopy (FTIR) was performed using samples of the BADCy cyanate-ester cured on polished aluminium-alloy substrates. The conversion of the cyanate-ester functional groups to s-triazine rings can be monitored using FTIR via determining the ratio of the -OCN absorbance at 2272 cm^{-1} to the CH_3 stretching peak at 2874 cm^{-1} for the cured resin, and by comparison of this value to that for the monomer. The fractional conversion is given by [1 - (cured resin ratio/monomer ratio)] [17]. The almost complete disappearance of the peak at 2272 cm^{-1} indicated that nearly complete conversion was obtained and this was achieved when the final cure temperature for the resin was 260°C. Hence, the choice of 260°C as the final cure temperature, see Section 2.2. For such a cure schedule, the simple BADCy polymer possessed [10] a glass transition temperature, T_g, of 310°C, see Table II.

TABLE II Values of G_c (at 21°C) and T_g for the simple BADCy polymer and the co-reacted phenol-BADCy polymers

% Co-reacted phenol	Fracture energy, G_c, J/m^2	Glass transition temperature, T_g, °C [10]
0	150	310
5	135	260
10	220	228
15	320	201

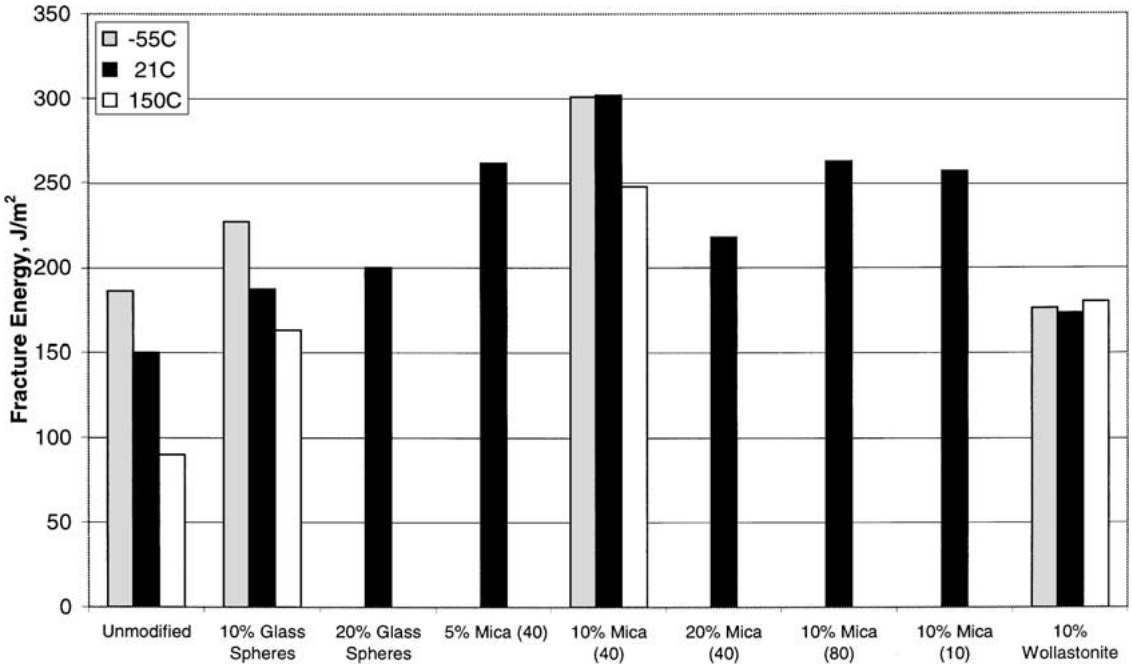

Figure 3 Fracture energies for the inorganic-particulate modified simple BADCy polymers, tested at −55, 21 and 150°C.

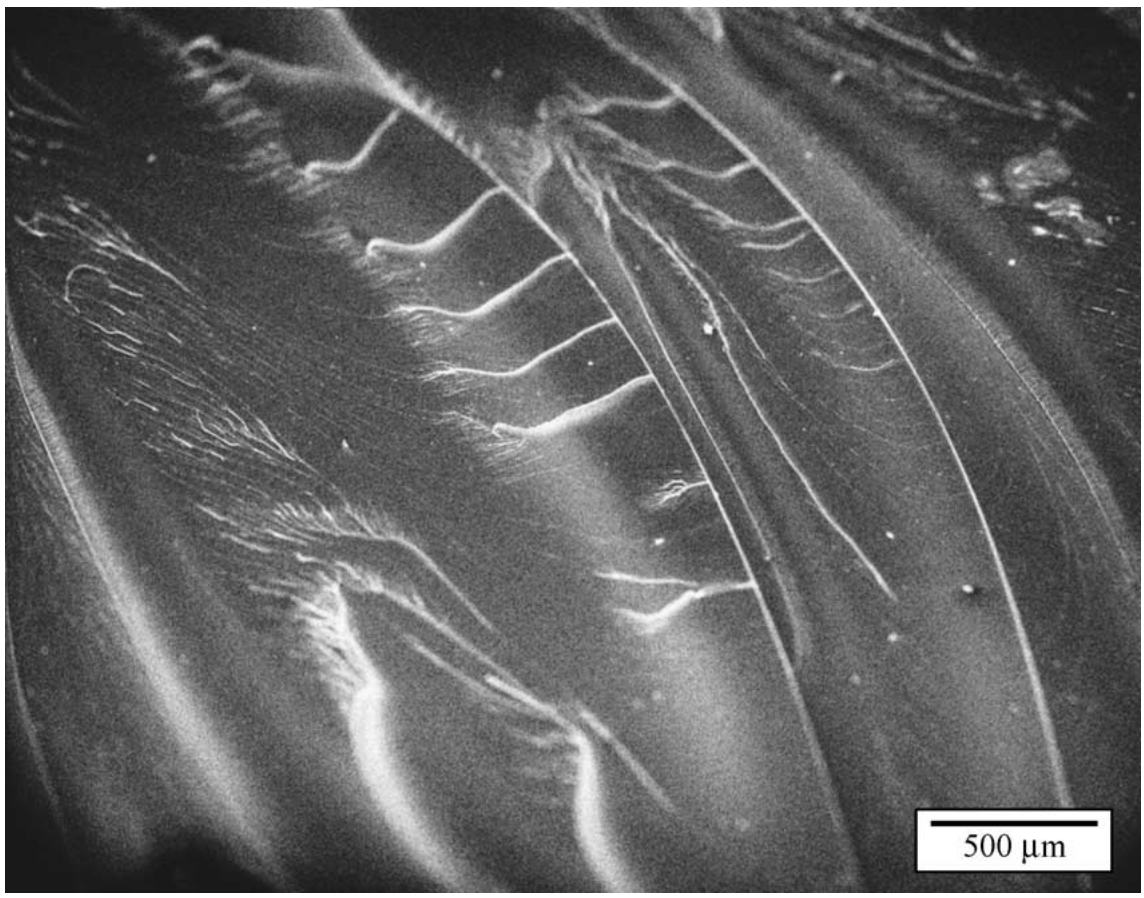

Figure 4 Fracture surface of unmodified simple BADCy polymer, tested at 21°C.

The TDCB specimens made with the simple, unmodified BADCy resin failed by stick/slip crack propagation, and a mean initiation fracture energy, G_c, value of 150 J/m^2 was measured at 21°C, see Table II and Fig. 3. A scanning electron micrograph of the fracture surface is shown in Fig. 4 and, as with all micrographs in the present paper, the crack propagation occurred from left to right. The micrograph shown in Fig. 4 illustrates features that are typical of the fast fracture associated with stick/slip crack growth in a very brittle material. The fracture surface of the unmodified BADCy polymer is relatively smooth and glassy, showing that little plastic energy dissipation has accompanied the fracture process. However, there are apparent steps and changes

of level of the crack. These features are feather markings, caused by the crack forking due to the excess of energy associated with the relatively fast crack growth. The multi-planar nature of the surface and this repeated forking are ways of absorbing this excess energy in a very brittle material [18].

The effect of test temperature on the simple, unmodified BADCy polymer was also investigated, and the fracture energy was found to decrease with increasing temperature, from 185 J/m^2 at −55°C to 90 J/m^2 at 150°C, as shown in Fig. 3. The crack growth was always via a stick/slip type of propagation, and the fracture surfaces were all relatively featureless.

3.3. Particulate-modified

3.3.1. Hollow glass spheres

Hollow glass spheres with a mean particle size of approximately 10 μm were used. The addition of these spheres at a 10% inclusion by weight increased the fracture energy of the BADCy polymer, at 21°C, from 150 J/m^2 to 187 J/m^2, as shown in Fig. 3. Further, the measured fracture energy of the BADCy polymer containing 10% by weight of the hollow glass spheres decreased steadily with increasing temperature, from 227 J/m^2 at −55°C to 163 J/m^2 at 150°C. However, it is noteworthy that at all temperatures the fracture energy was greater than that of the unmodified BADCy polymer. The addition of 20% by weight of the hollow glass spheres did not increase significantly the value of G_c measured at 21°C, compared to a 10% loading, again as may be seen from Fig. 3. It is noteworthy that the inclusion of the glass spheres resulted in the modified-polymers exhibiting stable crack growth, in contrast to the unmodified BADCy polymer which showed stick/slip crack growth.

3.3.2. Mica

Mica is a potassium aluminium silicate material [19] whose structure is composed of layers of stacked silicate flakes, see Fig. 5 for example. Three particle sizes were used in the present work, of mean particle sizes between 10 and 80 μm, as shown in Fig. 5. The particle sizes quoted are taken from the manufacturer's data [20]. Notwithstanding, the effect of particle size is small: the mean fracture energies at 21°C all lying within the standard deviation of about 20 J/m^2, as may be seen from the results given in Fig. 3. For example, a mean G_c value of 302 J/m^2 was measured for the polymer with 10% of the 40 μm mica, compared to about 260 J/m^2 for the other particle sizes at this concentration of added mica. Microscopy of the fracture surfaces of the mica-modified BADCy polymers showed that the mica flakes tend to lie relatively flat on the surface, as shown in Fig. 6, due to the spreading action used to apply the modified-resin to the substrates.

The effect of the concentration of added mica was studied using the mica with a mean particle size of 40 μm and a test temperature of 21°C. The effect of the level of added mica was not large, with the maximum fracture energy, of 302 J/m^2, being obtained at an inclusion level of 10%, see Fig. 3. Indeed, increasing the concentration of mica to 20% reduced the fracture energy to 218 J/m^2. The fracture energy of the BADCy polymer containing 10% mica, with a mean particle size of 40 μm, was relatively insensitive to temperature: values of 301 and 248 J/m^2 being measured at −55 and 150°C respectively.

3.3.3. Wollastonite

Wollastonite is a calcium metasilicate material [19] which has needle-shaped particles. The particles were typically about 50 μm long by 10 μm in diameter. When 10% of wollastonite was present in the BADCy polymer, a fracture energy of 170 J/m^2 was measured at 21°C, compared to 150 J/m^2 for the unmodified polymer. Tests at −55 and 150°C showed that there was little effect of test temperature on the fracture energy; values of 178 and 180 J/m^2 being measured at −55 and 150°C respectively. Thus, the addition of wollastonite appears to have little effect on the toughness of the unmodified cyanate-ester polymer, except at the highest test temperature of 150°C where it increases the toughness by a factor of about two compared to the unmodified polymer. These results are clearly illustrated in Fig. 3.

3.3.4. PTFE powder

The poly(tetrafluoroethylene) (PTFE) powder used was composed of irregular-shaped particles about 8 μm in diameter. Using a concentration of 10% of PTFE in the BADCy polymer led to crack propagation in a stick/slip manner, and a mean initiation fracture energy of 232 J/m^2 was measured at 21°C. This compares to a G_c value for the unmodified resin of 150 J/m^2. At −55 and 150°C, fracture was in a stick/slip manner, and fracture energies of 226 and 376 J/m^2, respectively, were measured. Thus, there is a large increase in the fracture energy at 150°C, especially compared to that of the unmodified polymer at this temperature, for which G_c was 90 J/m^2. Using a concentration of 30% of PTFE powder in the BADCy polymer did not lead to any significant further increases in the value of G_c at 21°C, and hence further tests were not undertaken at the other test temperatures. These data are shown in Fig. 7. The fracture surfaces of the PTFE-modified BADCy polymer appeared very similar at all the test temperatures. In Fig. 8 a micrograph of the fracture surfaces shows a relatively brittle failure of the polymer, with areas where PTFE particles have debonded from the matrix resin.

3.3.5. PEEK powder

Poly(ether-ether ketone) (PEEK) powder with a particle size of about 100 μm was used, again the particles possessed an irregular-shape. At a concentration of 10% of the PEEK powder, a fracture energy of 250 J/m^2 was measured, compared to a value of 150 J/m^2 for the unmodified BADCy polymer, see Fig. 7. There is little effect of the test temperature for the BADCy polymer containing 10% PEEK powder, the mean fracture energies remaining within the standard deviation of about ±15 J/m^2. Increasing the concentration of the PEEK powder in the BADCy polymer increases the fracture energy at 21°C to 295 J/m^2 at 20% concentration of PEEK powder and to 470 J/m^2 at 30% of PEEK powder.

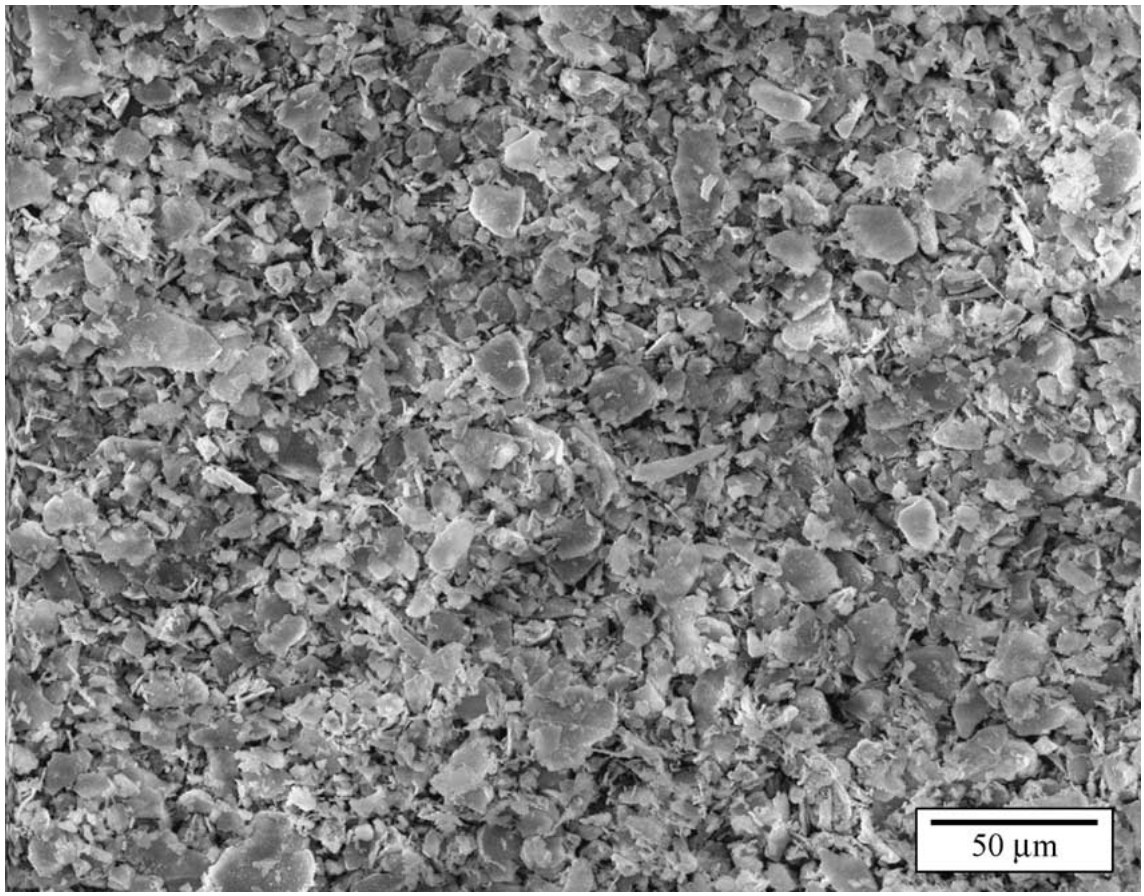

(a)

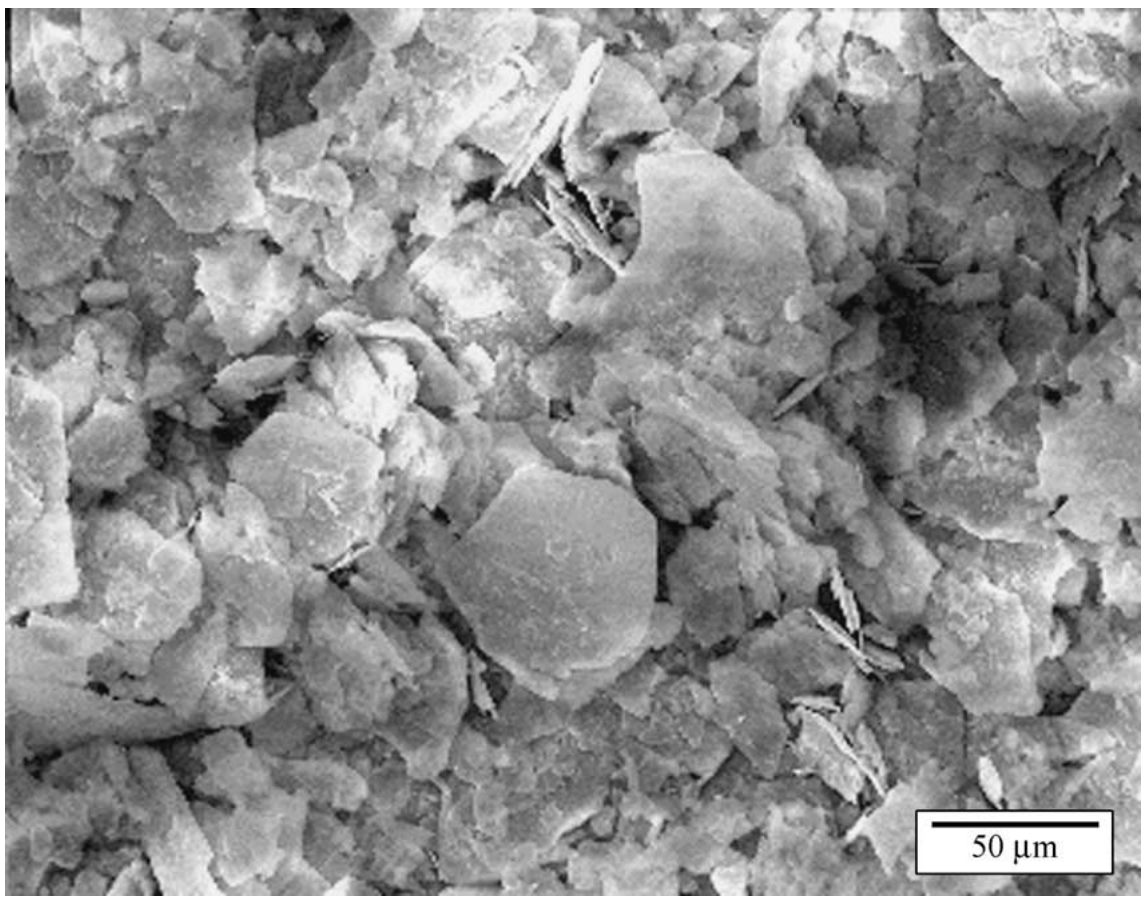

(b)

Figure 5 Mica types used in the present work: (a) mica (SX400) of mean particle size 10 μm, (b) mica (P66) of mean particle size 40 μm, (c) mica (R120) of mean particle size 80 μm. (*Continued*.)

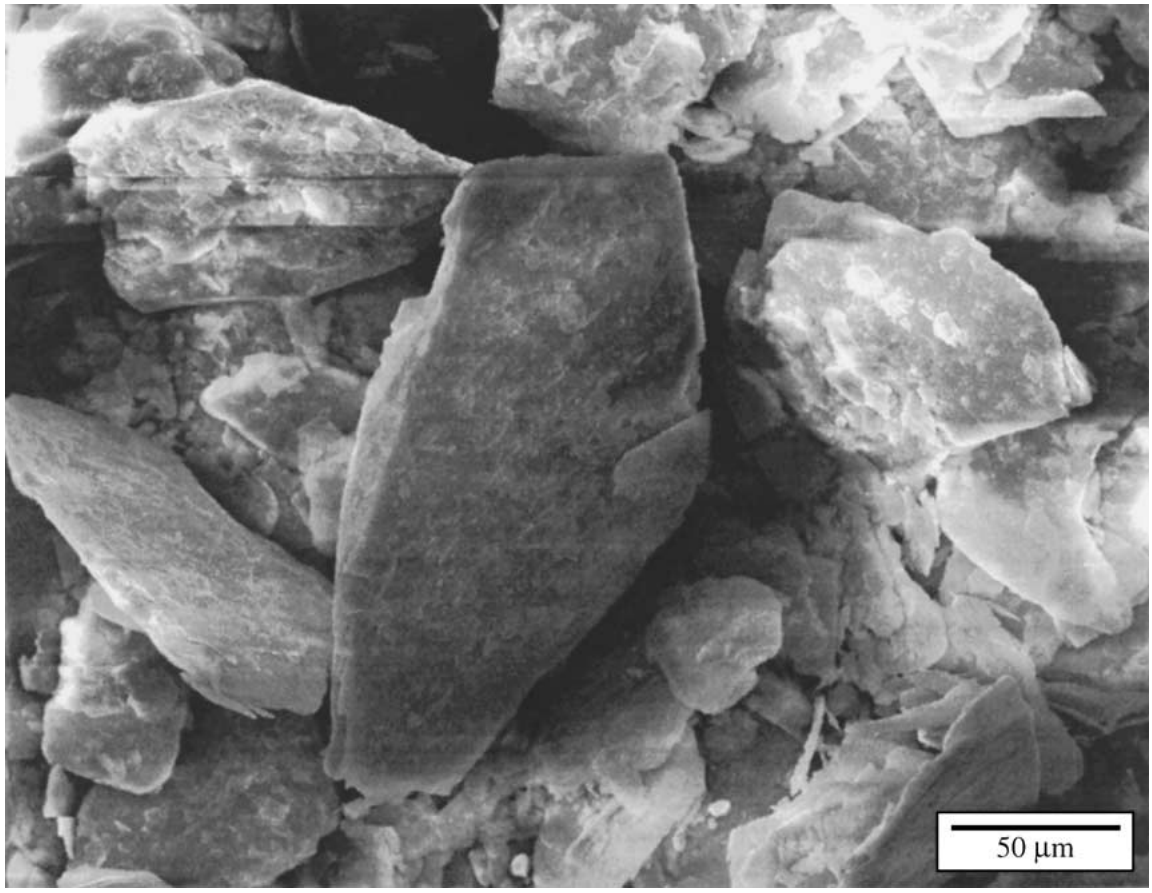

(c)

Figure 5 (*Continued*.)

However, the fracture energies are much less than those predicted from a rule of mixtures relationship. For example, at 20% by weight of PEEK, the rule of mixtures would predict a fracture energy of 2080 J/m^2 compared to an experimentally measured value of 295 J/m^2, assuming that the fracture energy of the PEEK polymer is 9800 J/m^2 [21].

3.3.6. Other particulate modifiers

The other particulate modifiers that were studied were alumina, silicon dioxide, titanium dioxide and yttrium oxide, and the results are listed in Fig. 9. As may be seen, none had any significant effect on increasing the toughness of the simple BADCy polymer when tested at 21°C. Thus, further tests at the other temperatures were not conducted. It was particularly noteworthy that the addition of nanometre-sized particulate modifiers had little toughening effect on the BADCy polymer, and actually tended to reduce the measured fracture energy, G_c. For example, at an inclusion level of 10% of TiO_2 in the BADCy polymer the fracture energy was reduced from a value of 150 J/m^2 for the unmodified polymer to 131 J/m^2 for the nano-particulate modified polymer.

3.3.7. Summary

From the values of G_c shown in Fig. 3, the most successful inorganic modifier was mica which at the optimum concentration of 10% by weight gave a fracture energy of 302 J/m^2 at 21°C, compared to 150 J/m^2 for the unmodified polymer. This value of G_c was not greatly affected by the test temperature. For example, a value of 248 J/m^2 was recorded at 150°C, which is a major increase compared to the value of 90 J/m^2 for the unmodified BADCy polymer at this temperature. Also, there was no significant effect of the particle size of the mica upon going from a mean particle size of 10 μm to 150 μm. The inclusion of nanometre-sized particles all tended to reduce the measured fracture energy compared to that of the unmodified BADCy polymer, see Fig. 9. Considering the organic-particulate modifiers, see Fig. 7, the addition of PTFE particles resulted in a large increase in the measured fracture energy at 150°C due to softening of the PTFE. The addition of 10% of PEEK particles to the unmodified BADCy resin also gave a significant increase in the fracture energy to about 250 J/m^2. However, this value was relatively insensitive to the test temperature. This is as expected, since the properties of PEEK are less temperature dependent than those of PTFE over the temperature range currently employed.

3.4. Fibre and woven-mat modified

3.4.1. Carbon short-fibres

Carbon fibres, 7 μm in diameter and 1 mm long were incorporated in the unmodified BADCy resin at 10% by weight, which is equivalent to a volume fraction of 5.9%. The fibres tended to aggregate together, but careful joint preparation ensured that the fibres were relatively well wetted by the molten resin. At 21°C, a mean G_c value of 195 J/m^2 was measured, as may be seen for the results given in Fig. 10. Thus, compared to the G_c value of 150 J/m^2 for the unmodified BADCy

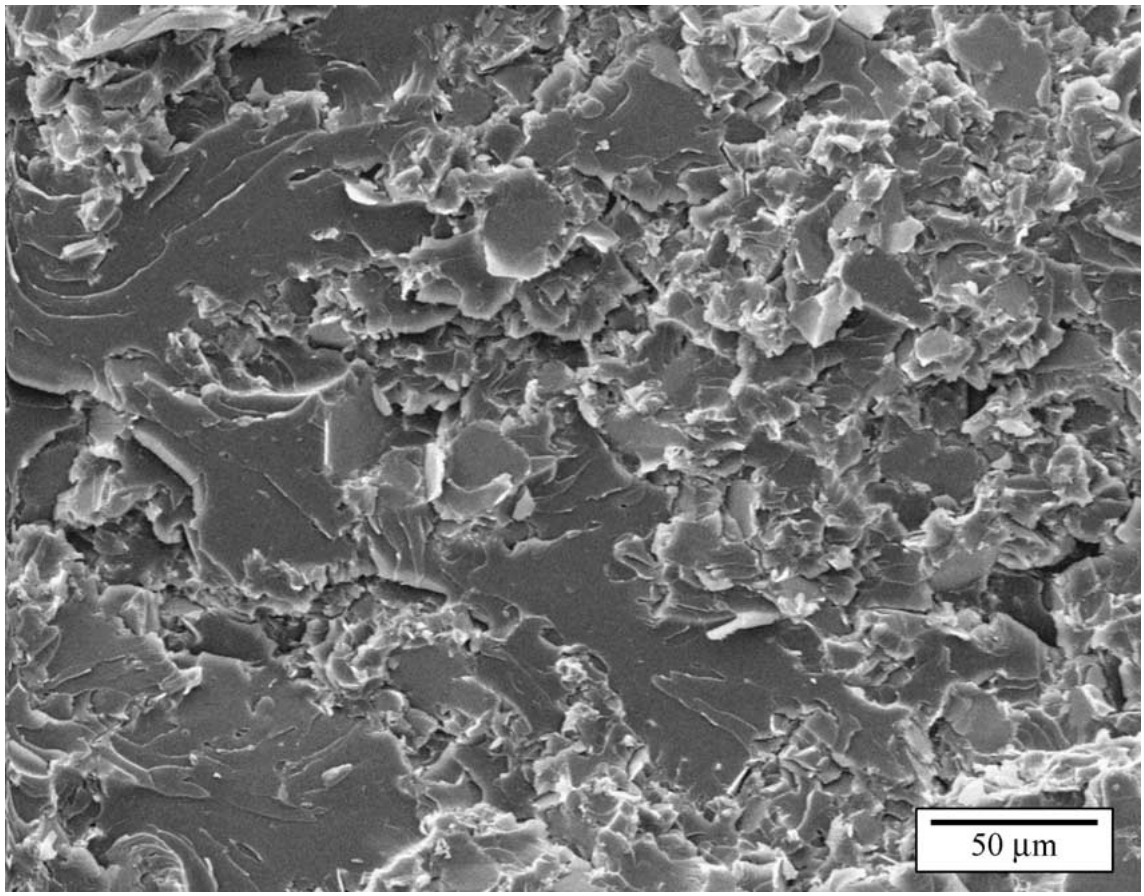

(a)

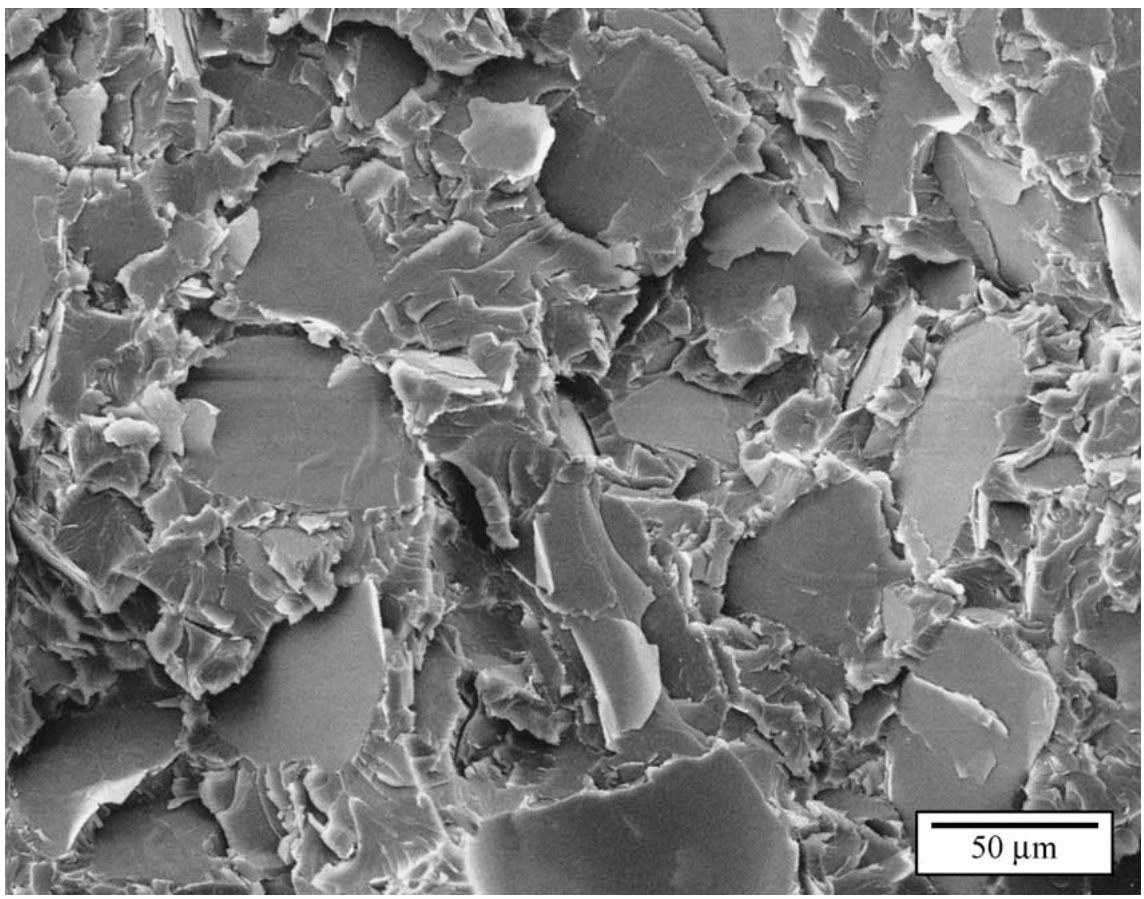

(b)

Figure 6 Fracture surfaces of simple BADCy polymer modified with 10% of mica: (a) mica (SX400) of mean particle size 10 μm, (b) mica (P66) of mean particle size 40 μm, (c) mica (R120) of mean particle size 80 μm, tested at 21°C. (*Continued.*)

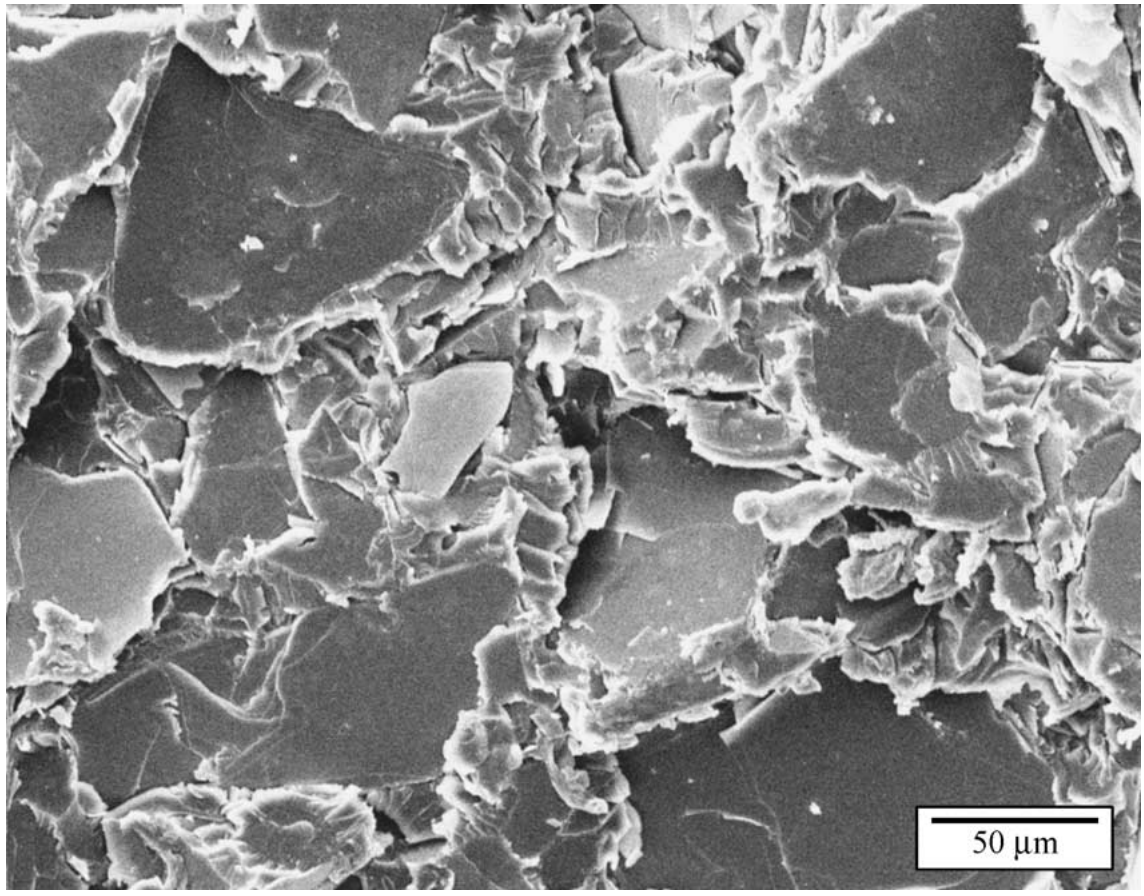

(c)

Figure 6 (*Continued*.)

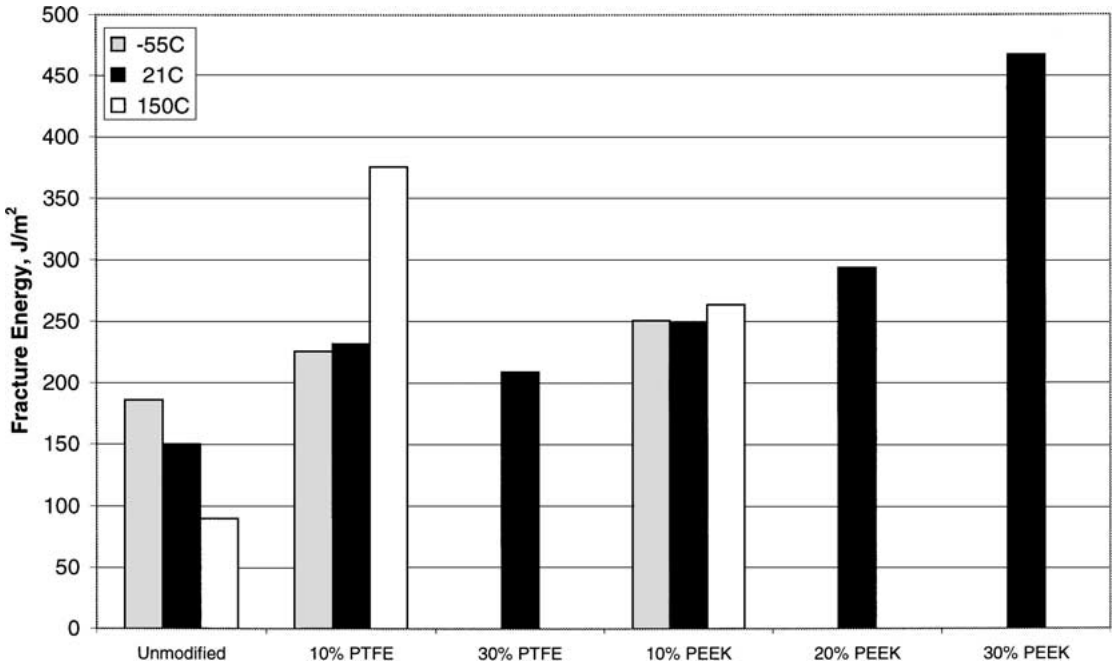

Figure 7 Fracture energies for the polymeric-particulate modified simple BADCy polymers, tested at −55, 21 and 150°C.

resin, the addition of carbon short-fibres only imparts a slight improvement in the toughness of the BADCy polymer.

3.4.2. Kevlar short-fibres

The Kevlar short-fibres were difficult to handle and disperse through the resin, as they tended to aggregate strongly together. They were added at a concentration of 10% by weight (≡8.9% by volume). The fibres were not straight like the carbon short-fibres, but had a structure that was more three-dimensional. Thus, it was difficult to ensure that the resin properly wetted all the fibres. However, even with insufficient wetting, a value of G_c of 193 J/m^2 was measured at 21°C for initiation at short crack lengths; with a significant R-curve being observed which increased the value of G_c to 536 J/m^2. The

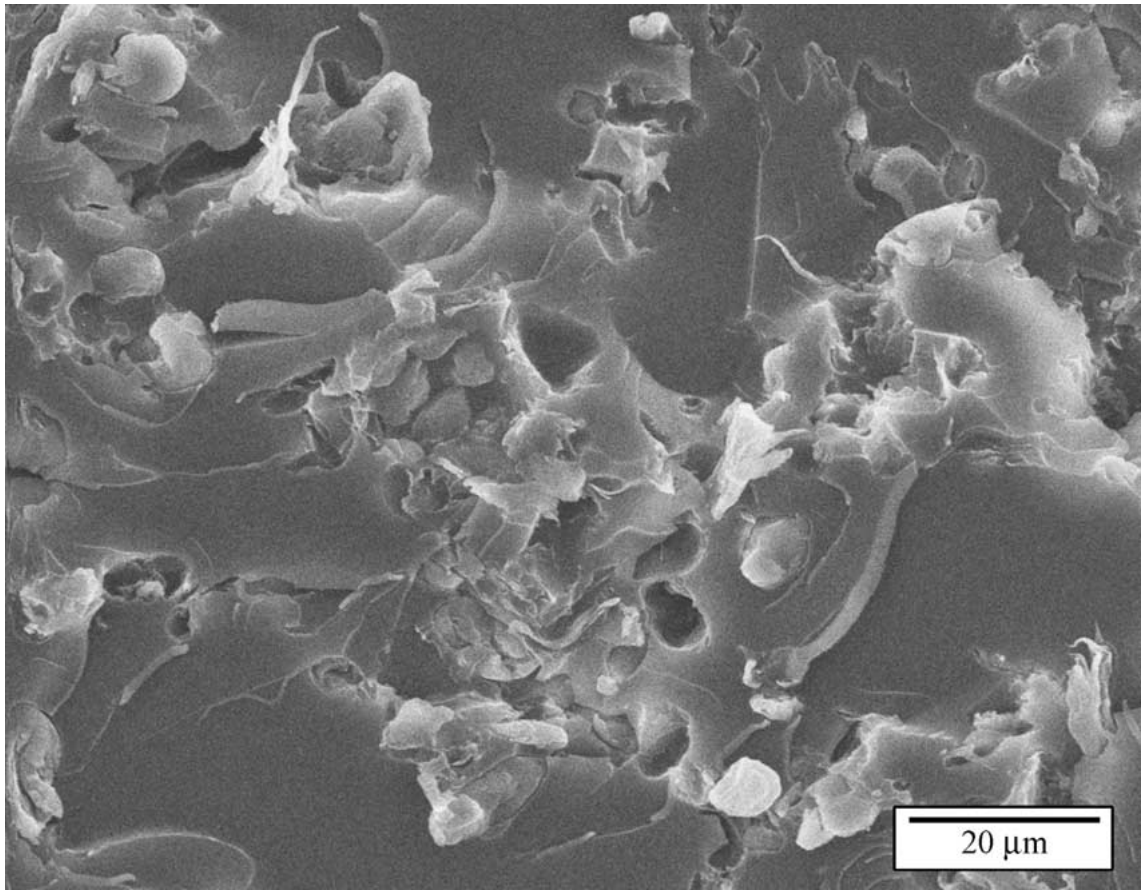

Figure 8 Fracture surface of simple BADCy polymer modified with 10% PTFE powder, tested at −55°C.

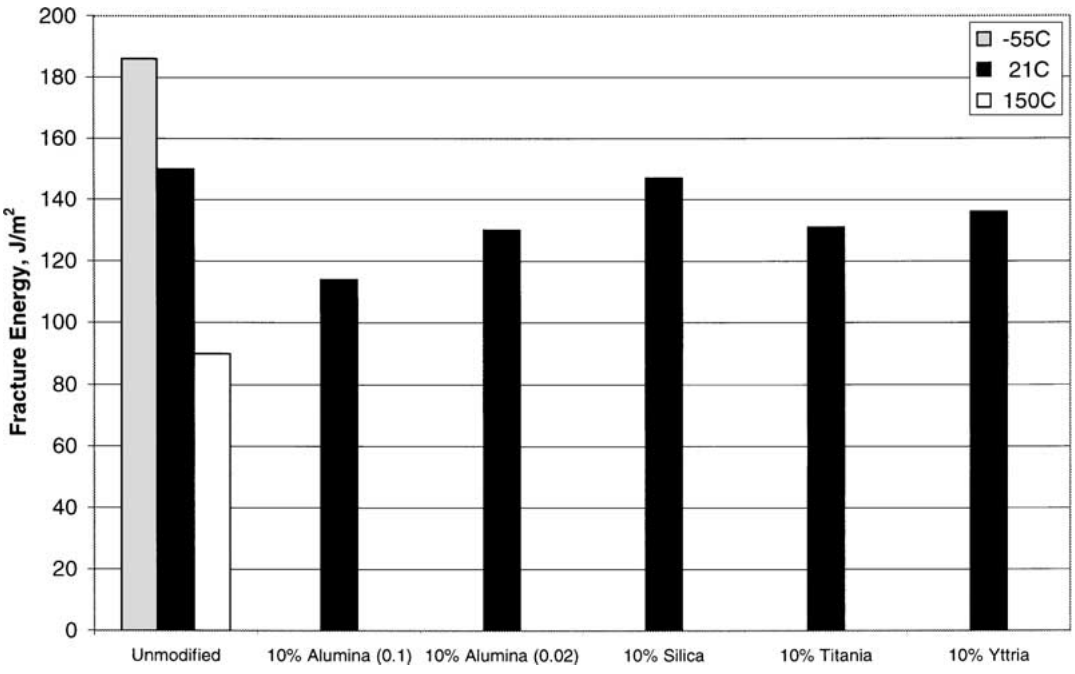

Figure 9 Fracture energies for the nano-particulate modified simple BADCy polymers, tested at −55, 21 and 150°C.

R-curve was clearly due to the fibres bridging across the fracture surfaces behind the crack tip that was advancing through the material, with associated debonding and stretching of the fibres occurring.

3.4.3. PEEK monofilaments

PEEK monofilaments, 200 μm in diameter and 320 mm long, were laid along the full length of the TDCB specimens, parallel to the direction of crack propagation. Eight monofilaments were used across the 10 mm width of the joints, although fewer were present in the finished joints as some were squeezed out when the joints were made. The calculated nominal percentage of monofilaments was 2.6 w/w%, which gives an equivalent volume fraction of 2.5%. The addition of the monofilaments did not significantly increase the fracture energy of the BADCy polymer, as may be seen from the results given in Fig. 10. Also, although the monofilaments pulled out

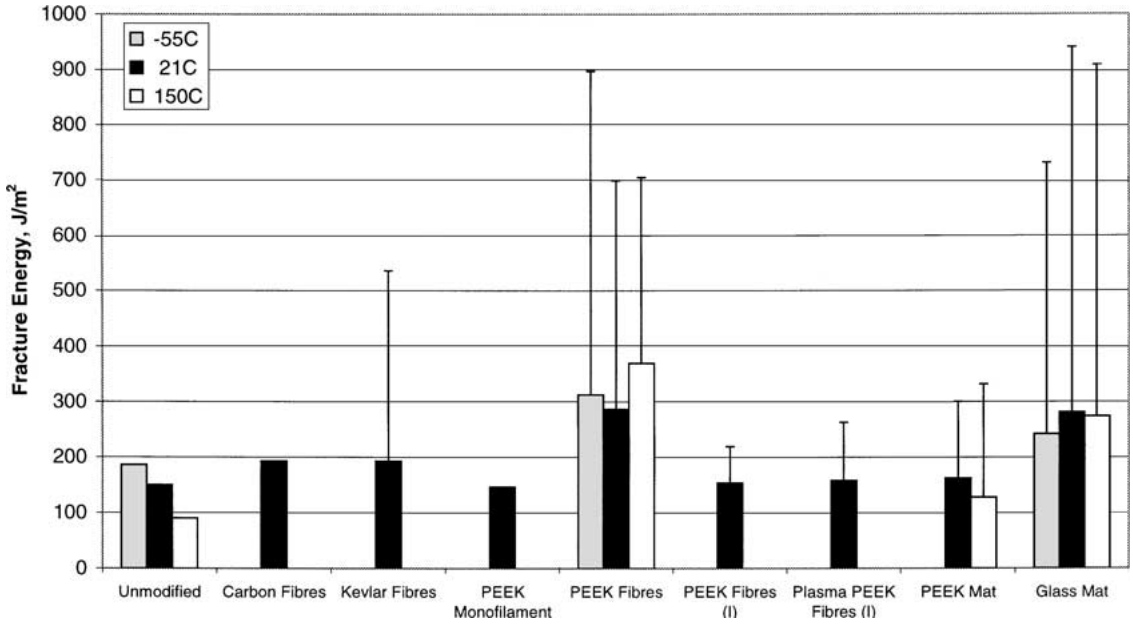

Figure 10 Fracture energies for the fibre and woven-mat modified simple BADCy polymers, tested at −55, 21 and 150°C. The column represents the fracture energy measured for crack initiation and the bar represents the maximum value of any *R*-curve observed.

and bridged across the fracture surfaces, no *R*-curve was observed. The crack propagation through the modified polymer occurred partly in a stable and partly in a stick/slip manner. From the fractographic studies, the cyanate-ester polymer clearly did not adhere to any significant degree to the PEEK monofilaments, and failure occurred cleanly at the monofilament/BADCy polymer interface.

3.4.4. PEEK fibres

Tows of PEEK fibres were laid along the length of the TDCB specimen, parallel to the direction of crack propagation. The fibres were 25 μm in diameter and 320 mm long. Eight tows of fibres were used across the 10 mm width of the joints and their nominal weight fraction was 6.7 w/w%, which is equivalent to a volume fraction of 6.5%. Testing at 21°C gave a fracture energy at crack initiation of 286 J/m^2. However, a very pronounced *R*-curve was observed, the fracture energy increasing to 699 J/m^2 at a crack length of 200 mm, see Fig. 10. During testing, the fibres were observed to debond from the resin and bridge extensively across the fracture surfaces. Indeed, after testing was complete and a crack had grown completely though the polymer, the fibres still bridged across the fracture surfaces and had to be cut with a knife to separate the two halves of the TDCB specimens. The simple BADCy polymer modified by the inclusion of the PEEK fibres was also tested at −55 and 150°C. Again pronounced *R*-curves were seen at both test temperatures, the fracture energies being equal to or slightly higher than those measured at room temperature, as may be seen from Fig. 10. The scanning electron micrographs of the fracture surfaces clearly revealed that, even at −55°C, the fibres had extensively debonded and pulled out from the BADCy polymeric matrix during the fracture process. The microscopy studies also revealed that failure occurred at the fibre/matrix interface, with virtually no polymer left adhering to the fibres themselves.

3.4.5. Plasma-treated PEEK fibres

From the above results, it was considered that if the PEEK fibres were surface treated, e.g. using a plasma treatment, to improve the adhesion then the fracture energy of the resulting physically-modified BADCy polymer may be increased further. Tows of PEEK fibres were therefore plasma-treated for 120 seconds at 100 Watts in an oxygen atmosphere. As expected [22], micrographs of the treated and untreated fibres prior to bonding showed no obvious differences, although the plasma treatment is known to chemically change the surface nature of the PEEK and so increase its surface free energy. Hence, it should be more readily wetted by, and adhere better to, the cyanate-ester resin. The tows of fibres were laid along the length of the TDCB specimens, parallel to the direction of crack growth. Eight tows of fibres were used across the 10 mm width of the joints, although fewer tows were present in the finished joints than in Section 3.4.4 above, as more tows were squeezed out of the bondline during manufacture. Indeed, the calculated percentages of fibres were 2.2 w/w% for the plasma-treated fibres, and 6.7 w/w% for the specimens in Section 3.4.4 above. Hence, to enable a valid comparison to be made, control specimens were prepared using the same number of tows, but employing the untreated fibres.

The results for the control specimens (denoted by 'PEEK Fibres (I)') are shown in Fig. 10. The lower concentration of the PEEK fibres has resulted in a significant decrease in the mean value of G_c, as may be seen by comparing the results at 21°C for the 'PEEK Fibres' and 'PEEK fibres (I)' specimens. For the 'PEEK Fibres (I)' specimens an *R*-curve was observed with the mean fracture energy rising from 155 J/m^2 at crack initiation to a maximum measured value of G_c of 220 J/m^2 at relatively long crack lengths. For the plasma-treated fibres (denoted by 'Plasma PEEK Fibres (I)'), a small increase in the values of G_c was observed; the fracture energy at crack initiation being 158 J/m^2 and rising to

a maximum value of 263 J/m^2. Thus, the plasma treatment of the fibres obviously has little effect on the measured fracture energies. This was in agreement with the results from the scanning electron microscopy studies of the fracture surfaces. These studies showed no obvious differences in the appearances of the failed surfaces between the specimens made using the untreated and plasma-treated fibres.

3.4.6. PEEK woven-mat

Specimens using BADCy polymer containing the PEEK woven-mat failed in a stable manner, with an R-curve showing an increase in the value of G_c from 162 J/m^2 at crack initiation to a maximum value of 300 J/m^2, see Fig. 10. Failure occurred along one surface of the woven-mat, which was not observed to bridge significantly across the fracture surfaces. Scanning electron microscopy, see Fig. 11, showed that little polymer is left adhering to the filaments of the mat, indicating that the adhesion of the resin to the mat is relatively poor. The increase in fracture energy with crack length is relatively small, i.e. the R-curve is not very pronounced. This is suggested to be due to poor adhesion, which causes debonding without bridging, and hence the R-curve is small. At 150°C, a maximum fracture energy of 333 J/m^2 was measured. Thus, as was observed when using the PEEK powder as a physical-modifier, there is only a slight increase in the toughening effect at higher temperatures, which may again be due to a very slight softening of the PEEK at 150°C. This may again be contrasted to the results from using the PTFE powder as a modifier, where a very significant increase in the value of G_c was observed at 150°C, see Fig. 7.

3.4.7. Glass woven-mat

Specimens were manufactured using the simple BADCy polymer containing a mat that consisted of woven tows of glass fibres, with a fibre diameter of 10 μm. A fracture energy of 233 J/m^2 was measured for crack initiation for these specimens at 21°C. However, a very pronounced R-curve was present, increasing to a maximum value of 940 J/m^2, see Fig. 10. It is suggested that the R-curve is more pronounced for the glass mat- than the PEEK mat-modified specimens due to the far better adhesion of the former to the polymeric matrix [2]. The glass woven-mat therefore debonds from the polymer matrix, but then can very effectively act as a load-bearing bridge across the fracture surfaces. As the crack propagates, further debonding occurs behind the advancing crack front causing additional energy dissipation, and hence the R-curve is relatively large. Micrographs of the fracture surfaces are shown in Fig. 12, and show that failure occurred at the glass-mat/polymeric-matrix interface. Fig. 12b shows that the glass woven-mat is virtually undamaged and has debonded from the BADCy polymer. The imprint of the mat appears on the opposite fracture surface, as shown in Fig. 12a.

At −55°C, values of the fracture energy somewhat lower than those at room temperature were measured, both for crack initiation and for the maximum measured value of G_c. However, the toughening effect of the glass

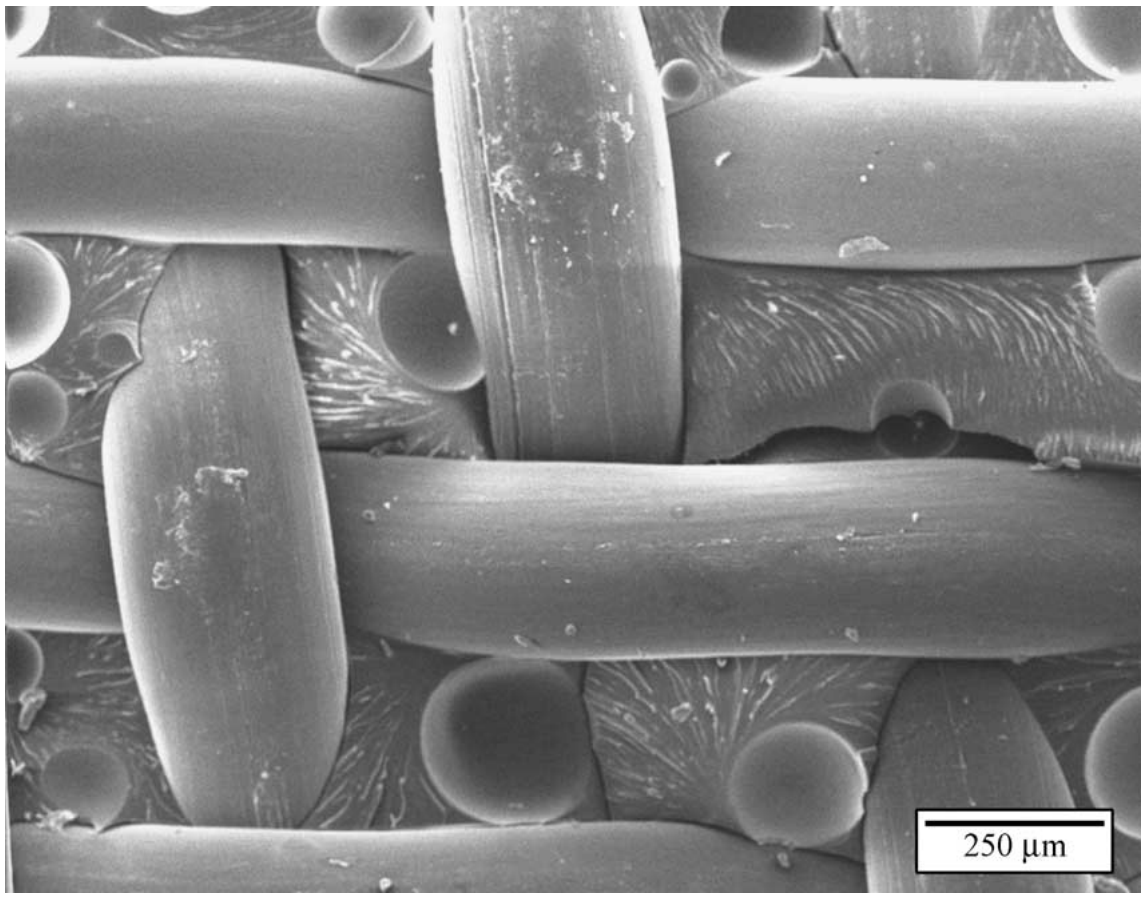

Figure 11 Fracture surface of the simple BADCy polymer modified with the PEEK woven-mat, tested at 21°C.

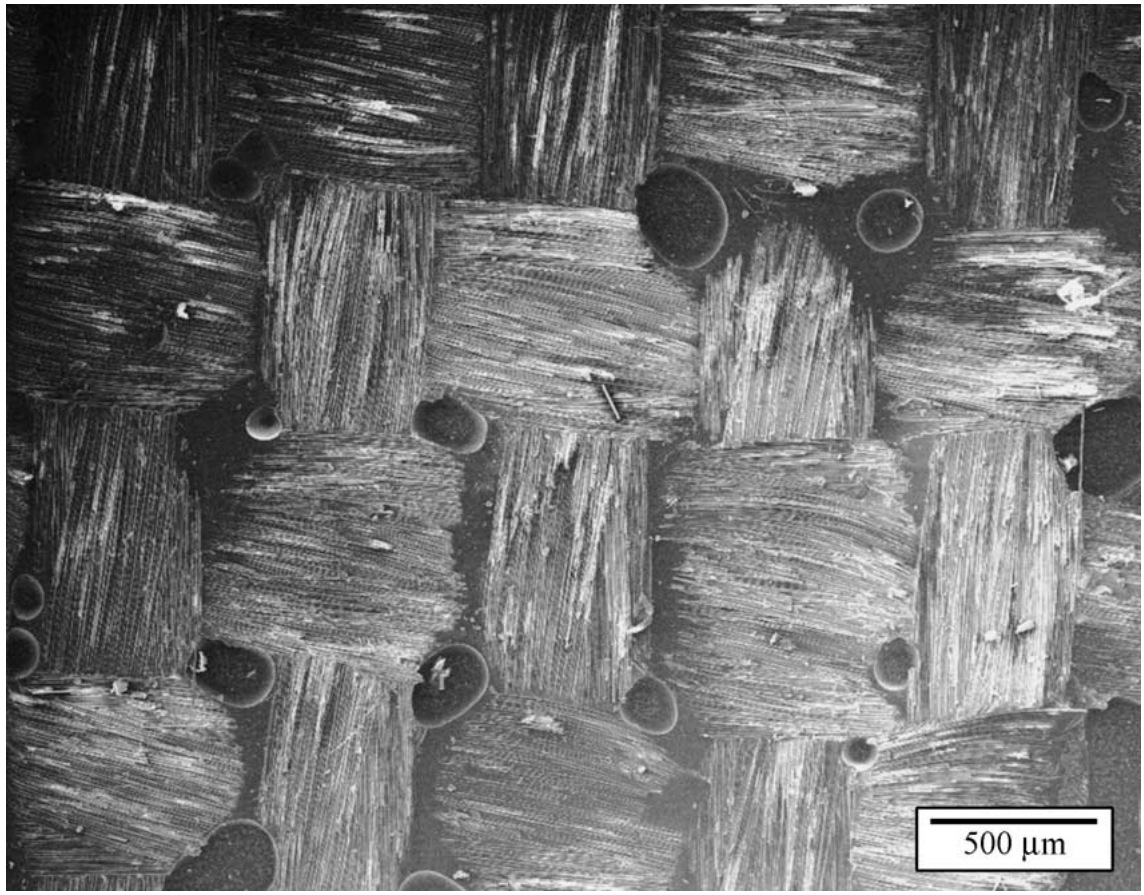

(a)

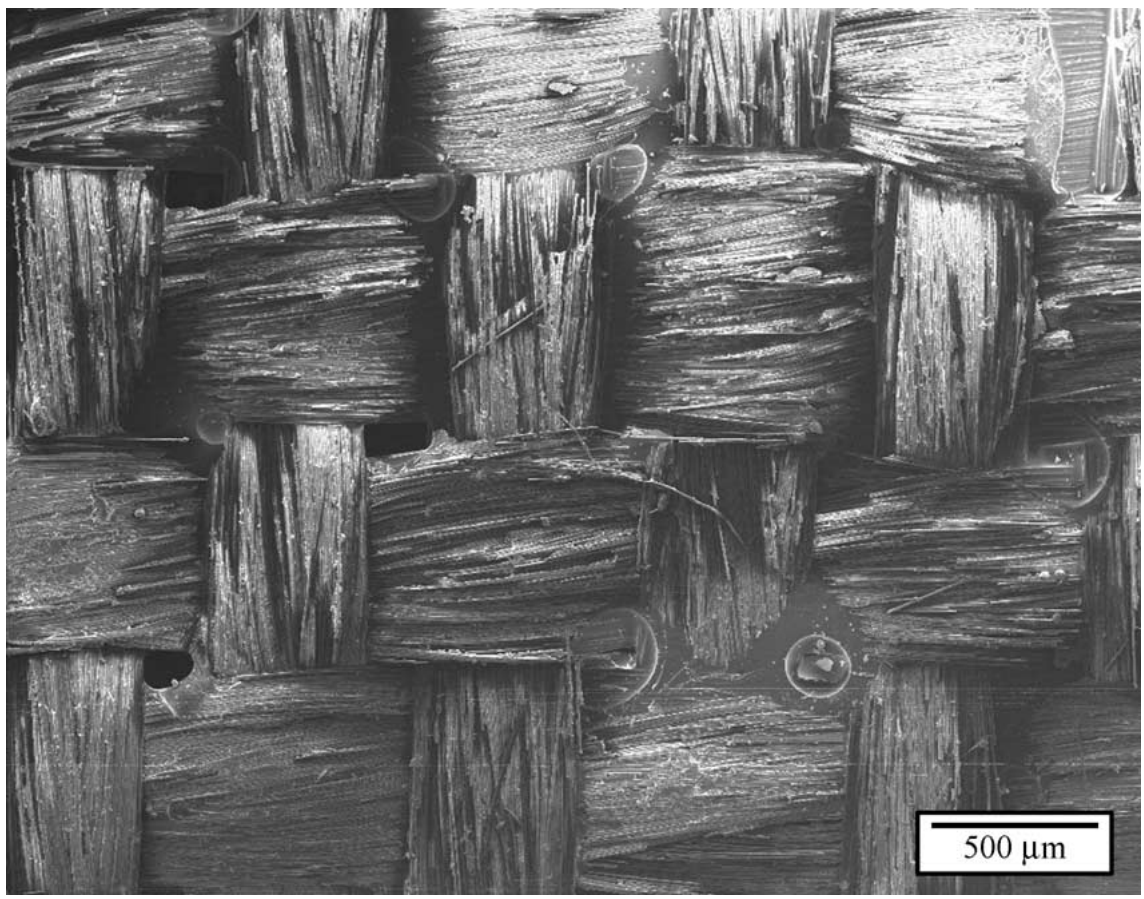

(b)

Figure 12 Fracture surfaces of the simple BADCy polymer containing the glass woven-mat tested at 21°C: (a) polymer side, and (b) mat side.

mat is still significant at all these test temperatures: the R-curve increasing to 731 J/m^2 at a crack length of 180 mm at −55°C. At 150°C, a significant R-curve was also seen, the fracture energies at initiation and at long crack lengths being approximately equal to the room temperature values, see Fig. 10. In all cases, crack growth occurred along the glass-mat/polymeric-matrix interface

4. Results and discussion: co-reacted phenol-BADCy polymers

4.1. Introduction

As discussed earlier, chemically-modified cyanate-ester polymers were produced with 5, 10 and 15% 4-cumylphenol co-reacted with the BADCy monomer. The measured fracture energies are summarised in Table II and Fig. 13. The value of the fracture energy at room temperature increases with a substantial increasing percentage of phenol: from 150 J/m^2 for the simple BADCy polymer to 320 J/m^2 for the co-reacted 15% phenol-BADCy polymer. However, whilst the addition of phenol increases the fracture energy of the cyanate-ester polymer, it also significantly reduces the glass transition temperature, T_g, as shown in Table II. Indeed, the T_g of the 15% phenol-BADCy polymer is only 200°C, which is a reduction of 110°C compared to the value for the simple BADCy polymer. Both of these features arise from the addition of the 4-cumylphenol, which increases the molecular weight between crosslinks of the cured polymer [7].

The effect of test temperature on the values of G_c is shown in Fig. 13. At −55°C, the fracture energy increases up to 10% of co-reacted phenol, but a reduction is observed at a level of 15%. At 150°C the values of G_c are similar to those measured at 21°C for both the 5% and 10% phenol levels. For the 15% phenol-BADCy polymer a value for the fracture energy could not be obtained at 150°C, due to plastic deformation of the aluminium-alloy substrates, which invalidates the linear-elastic fracture-mechanics analysis.

To limit the extent of the test programme for the research using the co-reacted phenol-BADCy polymers, the physical modifiers which were selected were those which had proven to be particularly successful when employed for the simple BADCy polymer, as described above.

4.2. PEEK powder

The inclusion of 10% by weight of PEEK powder in the 10% phenol-BADCy polymer gave a room temperature G_c value of 220 J/m compared to 250 J/m^2 for the simple BADCy polymer which also contained 10% PEEK, compare Figs 13 and 7. Thus the use of the 10% phenol-BADCy polymer, rather than the simple BADCy polymer (i.e. 0% phenol) does not significantly increase the measured fracture energy. The fracture surfaces for the PEEK-powder modified 10% phenol-BADCy polymer were very similar in appearance to those of the respective simple BADCy polymer.

4.3. Mica

The inclusion of 10% by weight of mica (mean particle size of 40 μm) to the 10% phenol-BADCy polymer gave a G_c value of 250 J/m^2 at 21°C, compared to 300 J/m^2 for the simple BADCy polymer containing 10% mica. Thus, the use of the 10% phenol-BADCy, rather than the simple BADCy, polymer actually reduces somewhat the value of G_c, as may be seen from comparing the data shown in Figs 3 and 13. The fractographic studies showed that the fracture surfaces were very similar for the two types of polymers containing 10% mica.

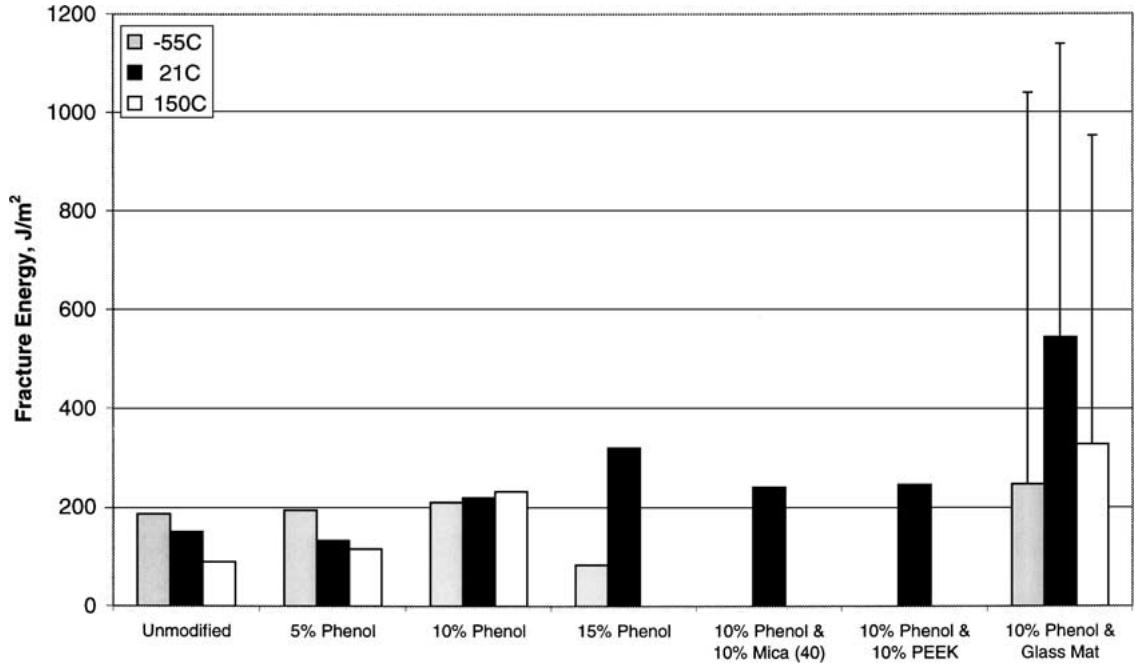

Figure 13 Fracture energies for the unmodified simple BADCy polymer and the co-reacted phenol-BADCy polymers with and without the inclusion of various physical modifiers, tested at −55, 21 and 150°C. The column represents the fracture energy measured for crack initiation and the bar represents the maximum value of any R-curve observed.

4.4. Glass woven-mat

Specimens were prepared using the 10% phenol-BADCy polymer containing the glass woven-mat. The values of G_c are given in Fig. 13. It may be seen that an R-curve was observed at all the test temperatures. The fracture energy for crack initiation at 21°C is 544 J/m^2 and is therefore considerably greater than the values of both the unmodified 10% phenol-BADCy polymer (i.e. 219 J/m^2) and the simple BADCy polymer containing a glass woven-mat (i.e. 233 J/m^2, see Fig. 10). Further, the values of G_c at relatively long cracks (i.e. values of G_c measured some way along the R-curve) attain values of around 1000 J/m^2 for the 10% phenol-BADCy polymer containing the glass woven-mat at all the test temperatures. Thus, the increase in fracture energy due to the co-reaction of 10% phenol with the BADCy monomer is greatly enhanced when the glass woven-mat is added. From visual observations during testing, the crack propagated in a very similar manner for the glass woven-mat specimens whether the simple BADCy or the 10% phenol-BADCy polymer was employed; see Fig. 12 for the fracture surfaces from the former specimen. Namely, for the 10% phenol-BADCy polymer containing the glass woven-mat, the crack also grew along the woven-mat/polymeric-matrix interface. The mat then debonded from the resin and bridged across the fracture surfaces behind the advancing crack tip to give rise to the very pronounced R-curve.

5. Comparison of results

The commercially-available cyanate-ester, Metlbond 2555G, is supported on a glass-fibre woven-mat carrier. The Metlbond 2555G has a T_g of 232°C [1]. Thus, its value of T_g is well below that of the simple BADCy polymer but of a similar value to that of the 10% phenol-BADCy polymer.

The Metlbond 2555G fracture specimens all failed by stable crack propagation with an R-curve being observed. The locus of failure for the TDCB specimens was along the interface between the cyanate-ester polymer and the mat carrier. An R-curve was observed at all the test temperatures and the results are shown in Fig. 14a–c for −55, 21 and 150°C, respectively. The R-curves for the Metlbond 2555G material are compared in these figures to the values which were discussed above for the simple BADCy and the 10% phenol-BADCy polymers, both modified using a glass-fibre woven-mat. As may be seen, at −55 and 150°C the values of G_c for the initiation of crack growth are somewhat similar for all three materials. However, the values of G_c for the modified simple BADCy and 10% phenol-BADCy polymers increase very rapidly as the crack propagates and the R-curve develops. Thus, far higher levels of toughness are attained for the last two polymers as the crack propagates through the polymer and fibre-bridging behind the crack tip develops. The order of toughness is: Metlbond 2555G < glass-mat modified simple BADCy < glass-mat modified and co-reacted 10% phenol-BADCy. For the last two materials this reflects, of course, the trend in the basic toughness of the matrix polymer, see Table II. At 21°C, this trend is still observed but there is also a relatively larger difference in the values of G_c for the crack initiation, see Fig. 14b.

Finally, it is noteworthy that the toughest of the above materials is the 10% phenol-BADCy polymer physically modified using the glass-fibre woven-mat. For example, at 21°C, this material has a mean initiation G_c value of 544 J/m^2 and this rises to over 1000 J/m^2 for the steady-state propagation value of G_c. This compares to values of about 175 J/m^2 and 300 J/m^2 respectively for the commercial Metlbond 2555G adhesive; and to 220 J/m^2 for the unmodified 10% phenol-BADCy polymer and 150 J/m^2 for the unmodified simple BADCy polymer. Further, the values for the woven-mat modified 10% phenol-BADCy polymer quoted above are not significantly decreased when the tests are conducted at 150°C.

6. Toughening micromechanisms

6.1. Particulate-modified polymers

The inclusion of the various particulate modifiers into the simple BADCy polymer all gave a toughening effect, i.e. caused an increase in the value of the fracture energy, G_c, with the exception of all the nanometre-sized particles. The addition of these nanometre-sized particulate modifiers caused reductions in the measured fracture energies, as may be seen in Fig. 9. The nanometre-sized particles tended to clump together to form loose aggregates about 20 μm in diameter, i.e. a thousand times the diameter of the individual particles, prior to mixing with the resin. These aggregates were not broken up during mixing, and the particles were not evenly distributed throughout the polymer. As the particles within the aggregates are very small and loosely attached, the aggregates were observed from the fractographic studies to offer very little resistance to crack propagation. Hence, the overall toughening effect of the nano-sized particles tended to be negative. Thus, one criterion for a toughening effect is that the particles do not aggregate together, but are well-dispersed throughout the matrix.

The larger, micron sized, particles did not aggregate and the inorganic-particulate (see Fig. 3) and the polymeric-particulate (see Fig. 7) modified BADCy polymers possessed higher values of G_c than the unmodified polymer. Observations of the fracture surfaces using scanning electron microscopy revealed that the fracture surfaces of the particulate-modified BADCy polymers were significantly rougher than those of the unmodified polymer and that the particles often had debonded from the matrix polymer giving rise to a cavity surrounding the particle. There was also some fractographic evidence for the advancing crack having been pinned by the particles. These observations reveal the main toughening mechanisms.

Firstly, the increase in surface roughness induced by the presence of the particulate-modifiers arises from the particles causing the crack front to deflect, tilt and twist as it reaches and passes around them [23, 24]. This is one of the main toughening mechanisms involved in increasing the fracture energy of the wollastonite- and mica-modified materials. For example, Fig. 15a shows a micrograph of the fracture surface of the simple

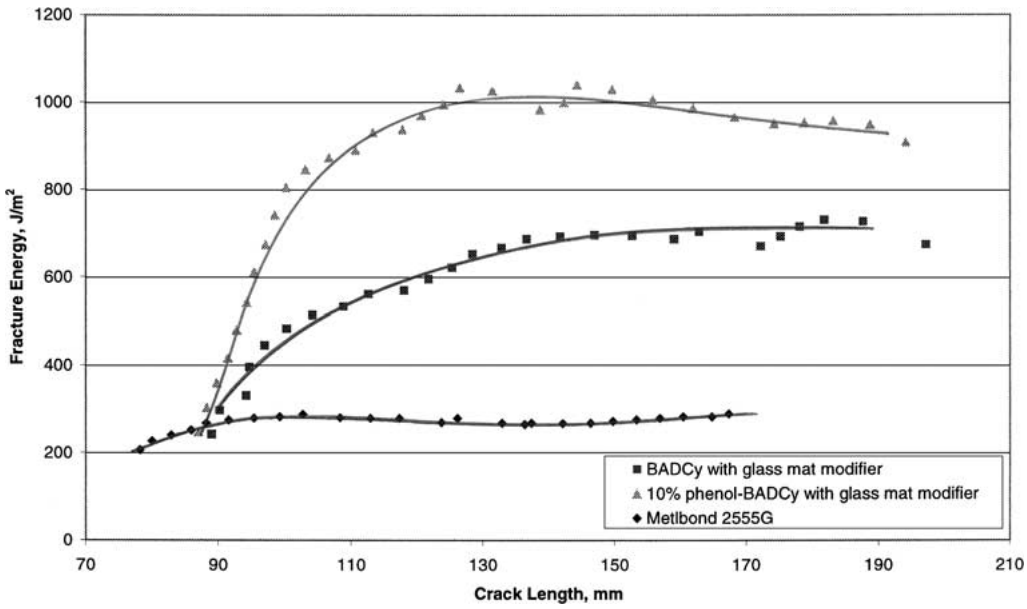

(a)

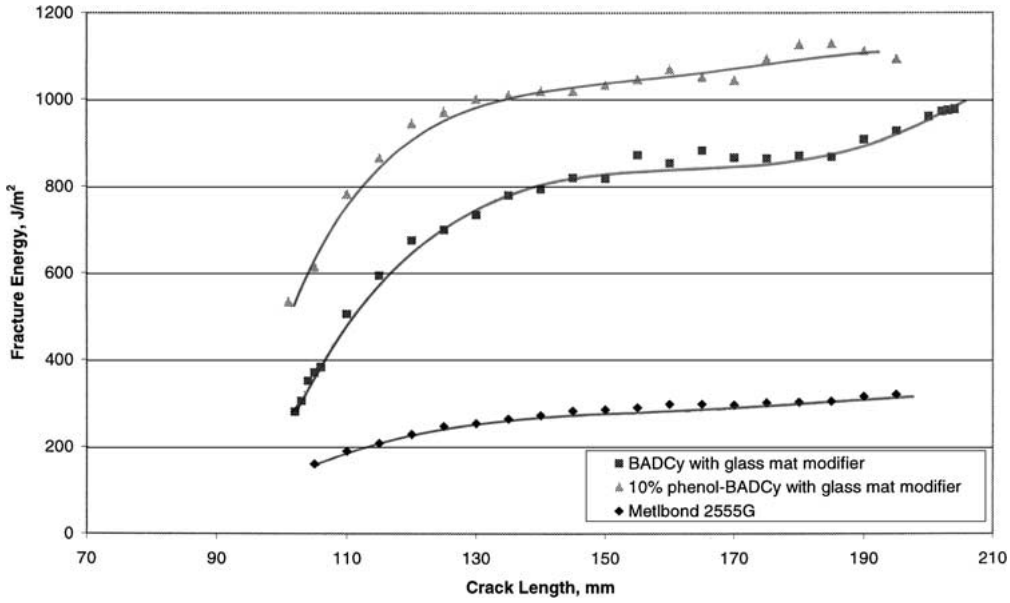

(b)

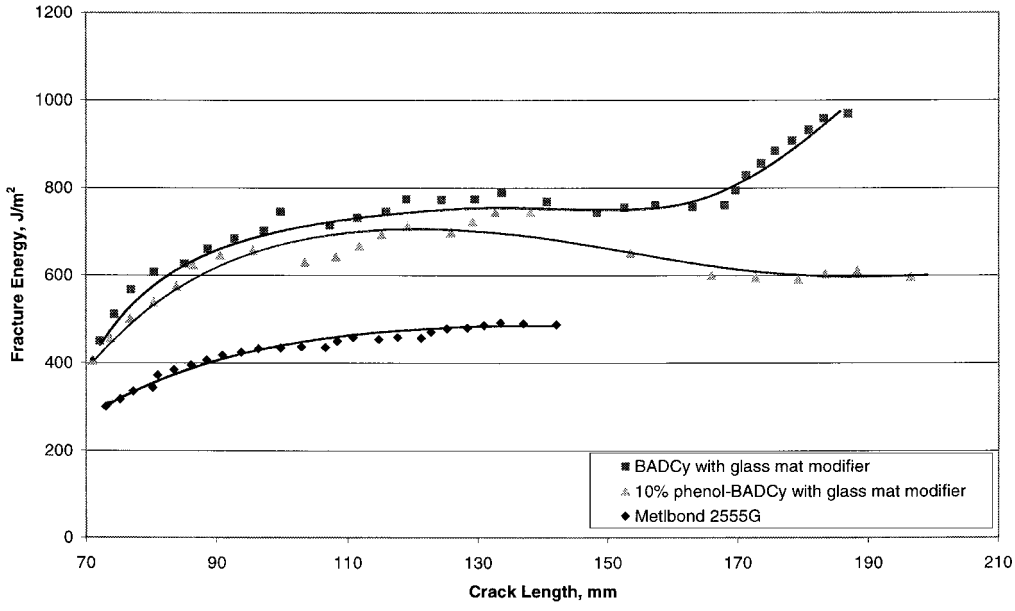

(c)

Figure 14 Fracture energy versus crack length for the woven-mat modified simple BADCy and 10% co-reacted phenol-BADCy polymers, and commercial film adhesive Metlbond 2555G: tested at: (a) −55°C, (b) 21°C, and (c) 150°C. Data from a single specimen are shown in each case.

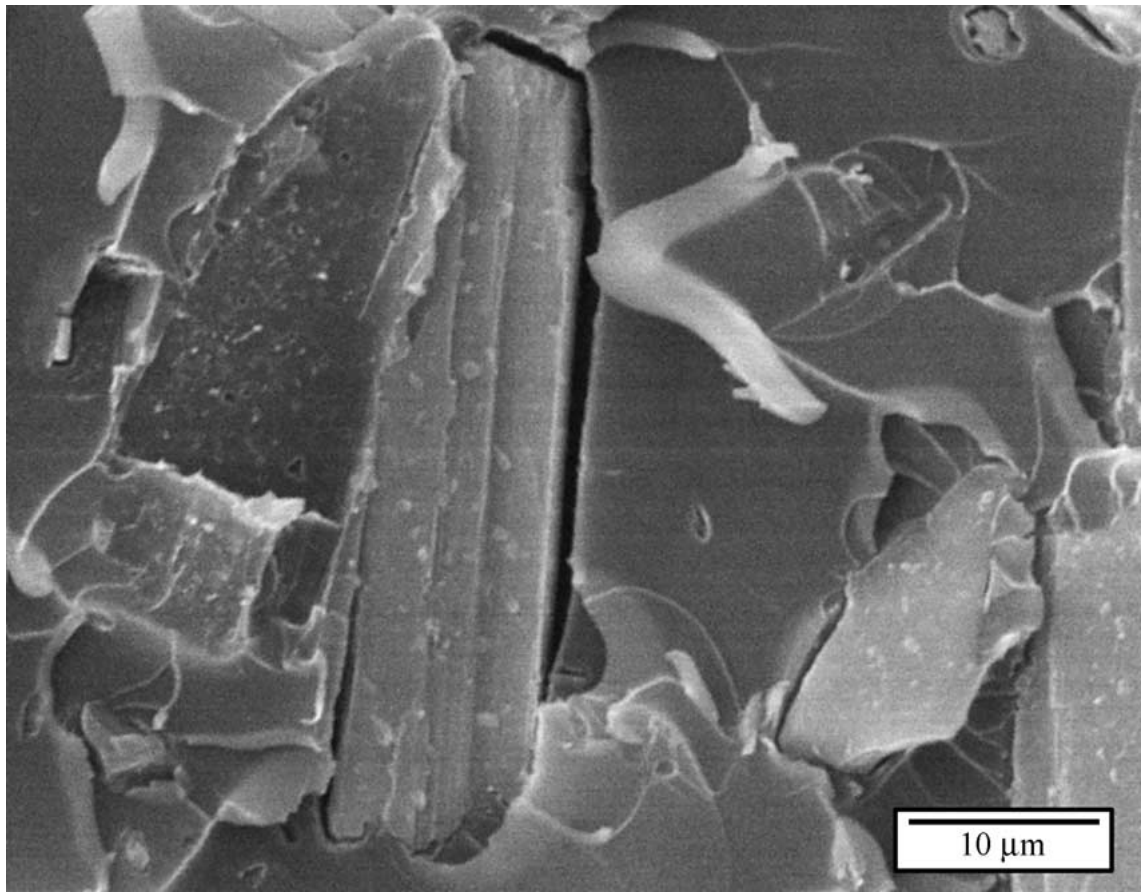

(a)

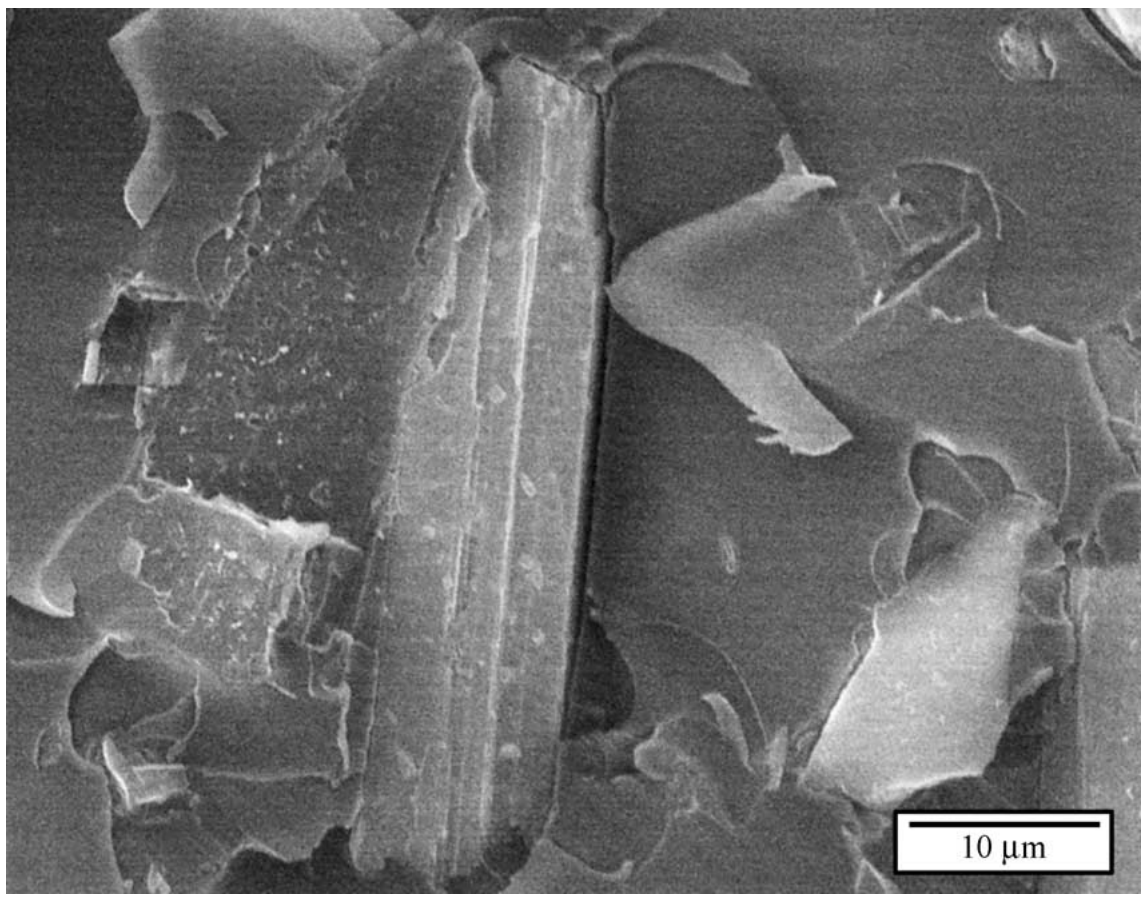

(b)

Figure 15 Fracture surface of simple BADCy polymer modified with 10% wollastonite tested at 150°C: (a) fracture surface, and (b) fracture surface after heating for 10 minutes at 10°C above T_g.

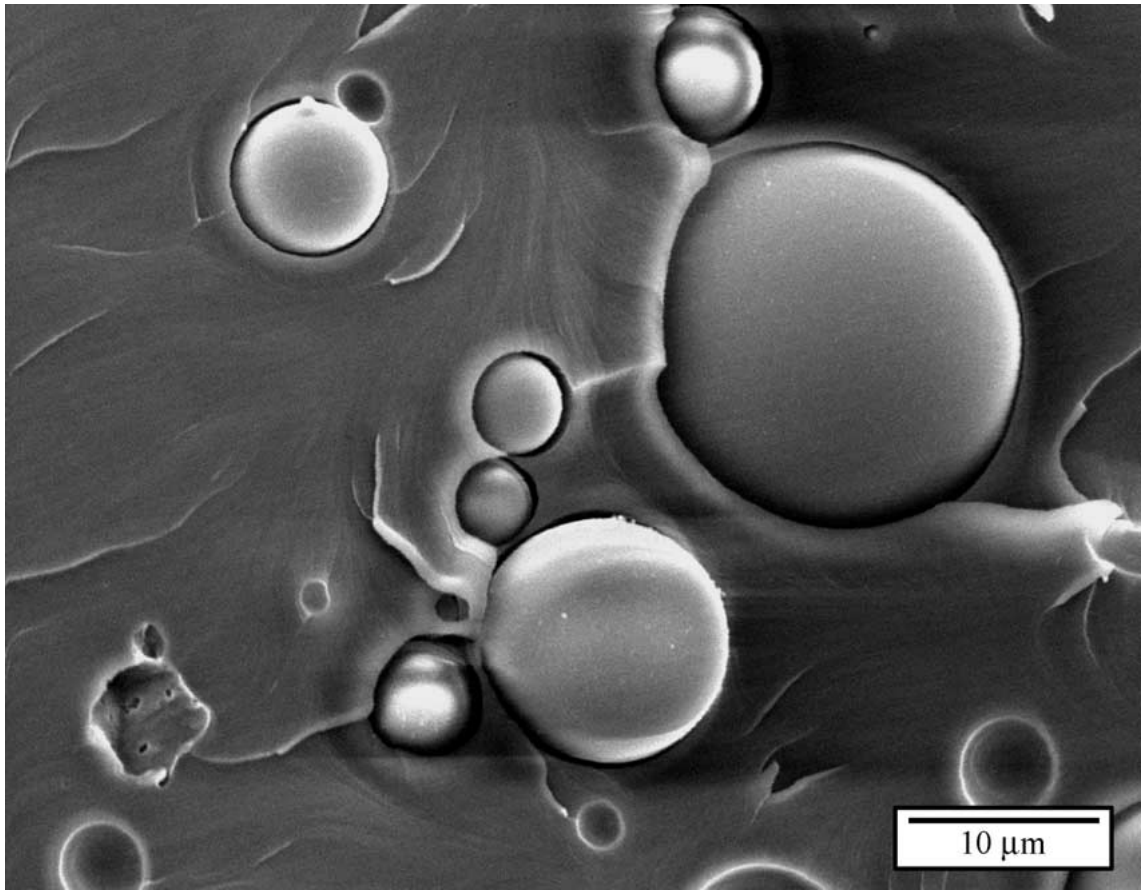

Figure 16 Fracture surface of simple BADCy polymer modified with 10% hollow glass spheres, tested at 21°C.

BADCy polymer modified with 10% wollastonite and, by comparison to Fig. 4, the greatly increased surface roughness is clearly evident. The needle-like and flake-like shapes, respectively, of these inorganic physical-modifiers clearly interfere with the smooth advance of the crack, causing the crack to deviate around the particles, and increasing the surface area of the fracture surface. However, it is noteworthy that the mica flakes tend to lie relatively flat on the fracture surface, see Fig. 6, due to the spreading action used to apply the modified-resin to the substrates when making the TDCB specimen. It is suggested that if the flakes could be orientated perpendicular to the direction of crack propagation, then the toughening effect may be significantly further increased.

Secondly, as noted above, cavities were observed around the particles after testing of some of the particulate-modified resins. For example, these may be seen clearly on the micrographs of the simple BADCy polymer modified with 10% of wollastonite and with 10% of 10 μm hollow glass-spheres, see Figs 15a and 16 respectively. These cavities might at first be considered to arise from differential thermal expansion of the resin and the particles during the cooling of the physically-modified polymer from its curing temperature down to room temperature. However, no cavities would be expected via this mechanism, since the polymer would contract more than the particles, hence ensuring that there were no cavities present around the particles. Indeed, inspection of the sides of the TDCB specimens prior to testing showed that no cavities were present prior to undertaking the fracture tests. Thus, the cavities around the particles must be formed during fracture of the specimens. It is suggested that the triaxial tensile stresses acting at the crack tip cause the particles to debond as the crack advances and that this debonding is followed by plastic hole growth of the polymeric matrix. Thus, the particles have the cavities surrounding them. The existence of plastic hole growth of the polymeric matrix was confirmed by heating the fracture surface of the wollastonite-modified BADCy resin for 10 minutes at 320°C, i.e. 10°C above the glass transition temperature of the resin. A comparison of the fracture surfaces before and after this heat treatment, see Fig. 15a and b respectively, shows that the cavities have closed up by relaxation of the plastically-deformed resin. It is suggested that the increase in G_c due to this toughening mechanism arises from the energy dissipated in the debonding of the particles and from that associated with plastic hole growth of the matrix. Cavitation around the particles was observed for the specimens modified using the hollow glass spheres, wollastonite, PEEK and PTFE particles. However, cavitation was only observed on the fracture surfaces of the PTFE-modified specimens tested at 150°C, whilst for the other particulate-modified polymers it was observed at all the test temperatures.

Thirdly, also as commented above, there was some evidence for crack-pinning. At the test temperature of −55°C, scanning electron microscopy of the fracture surfaces of the simple BADCy polymer modified with 10% hollow glass spheres showed that 'tails' were

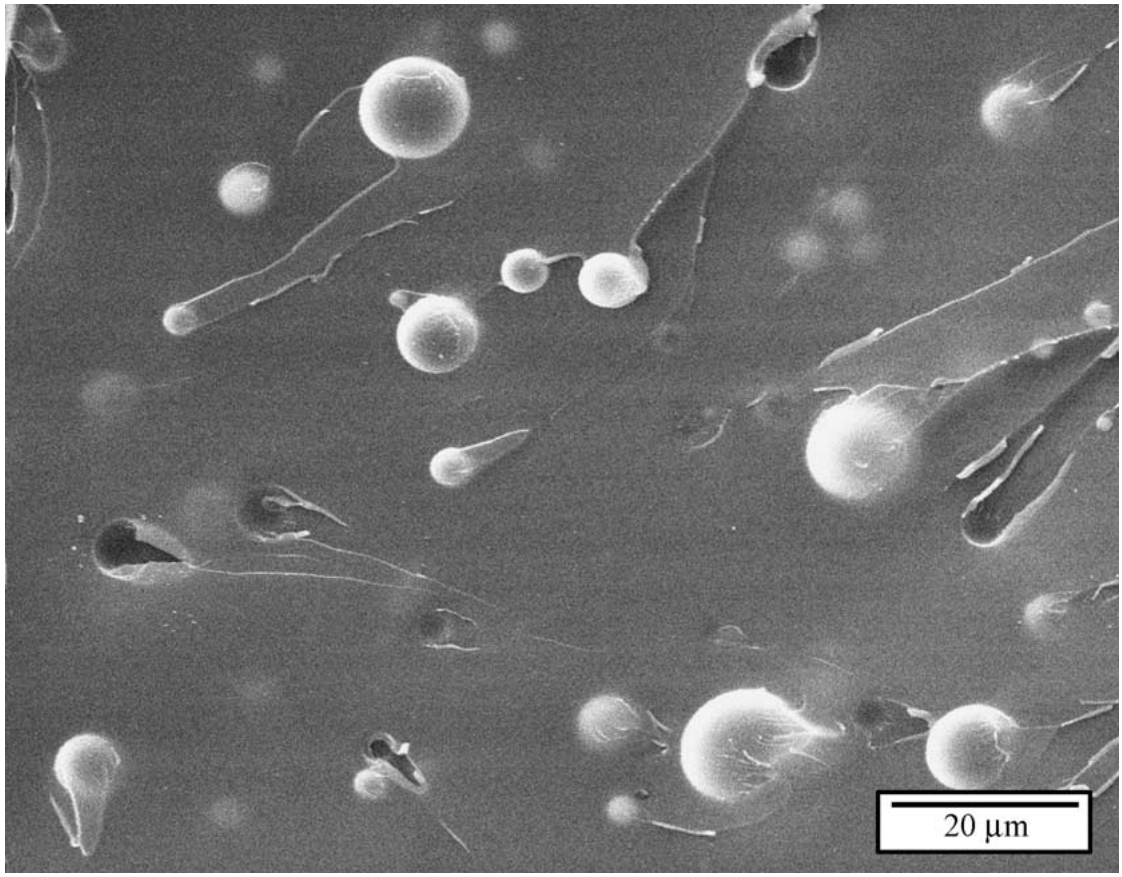

Figure 17 Fracture surface of simple BADCy polymer modified with 10% hollow glass spheres, tested at −55°C.

present at some of the glass spheres, see Fig. 17. The presence of such tails has been cited as evidence for crack pinning [25, 26], the tail being caused by the two sections of the pinned crack joining up. This crack pinning process may lead to an increase in the measured fracture energy for the modified resin. It should be noted that the tails are at different angles to the overall direction of crack propagation. However, fracture was in an unstable, stick/slip, manner. Hence, the local crack direction may be different from the global direction, due to local acceleration and deceleration of the crack front. Thus the tails, although parallel to the local direction of crack propagation, will not necessarily be parallel to the global direction.

Finally, in addition to the above toughening micromechanisms, there may be a contribution to the measured fracture energy due to the particles pulling-out of from the polymer. For example, microscopy of the fracture surfaces of the PTFE- and PEEK-modified polymers showed a relatively brittle failure of the polymers, with areas where the particles had pulled away from the matrix polymer; see for example Fig. 8. At −55 and 150°C, the fracture energy was greater for the PEEK-modified material than for the PTFE-modified material, see Fig. 7. This may be a function of either the particle size (i.e. 100 μm for PEEK and 10 μm for PTFE) or the properties of the physical modifier itself. However, for the PEEK-modified polymer there was no dramatic increase in the fracture energy at 150°C, unlike that seen with the PTFE-modified BADCy. This is in agreement with the observation that the PEEK softens less at 150°C than PTFE [27].

6.2. Fibre and woven-mat modified polymers

6.2.1. Introduction

All the modifications using fibres and woven-mats gave a toughening effect, and some caused an additional increase in the fracture energy with crack length, so as to give an R-curve when the fracture energy, G_c, is plotted versus the length of the crack as it propagates through the specimen.

Thus, it is useful to begin with an explanation of the presence and magnitude of the R-curves, as is shown schematically in Fig. 18. Firstly, consider the joint when no woven-mat or fibres are present. Here the measured fracture energy will be equal to that of the polymer. Secondly, consider a woven-mat (or fibres) that covers the entire resin surface, i.e. one with no holes between the tows of fibres (similar to the glass woven-mat used in the present work). If there is no adhesion between the mat and the resin, then it will act as a release film and a fracture energy of zero will be measured. If the adhesion is extremely good, then the bond between the polymer and the mat may be stronger than the cohesive strength of the polymer. Hence, the TDCB specimen will fail through the bulk of the polymer rather than at the mat/polymer interface. For intermediate levels of adhesion, the mat will give a toughening effect at initiation, similar to that given by the addition of particulate modifiers. As the crack grows, the mat will debond and effectively bridge across the fracture surfaces, leading to an R-curve. As the surface area of the mat in contact with the polymer is large, there is a large area that is capable of debonding, and hence the magnitude of the

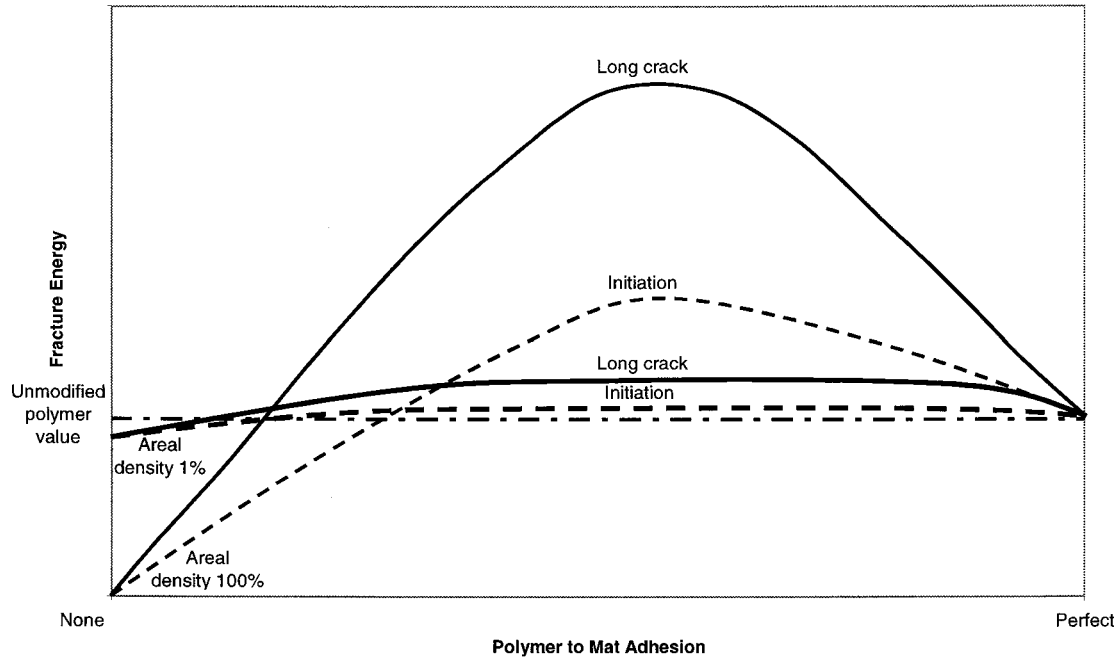

Figure 18 Schematic of fracture energy versus 'polymer to mat' adhesion for a woven-mat modified material. Values of G_c for initiation and for relatively long crack lengths (when any R-curve has developed) are shown for large (e.g. 100%) and small (e.g. 1%) areal densities of woven-mat.

R-curve will be large, see Fig. 18. Thirdly, consider the other extreme, namely a woven-mat (or fibres) where the material forming the mat (or the fibres) only covers a small percentage of the polymer surface. Once again, if the adhesion is perfect, then the TDCB specimen will fail through the polymer and the measured fracture energy will be equivalent to that of the polymer. However, if there is zero adhesion between the polymer and the mat, then a fracture energy only slightly lower than that of the polymer will be measured, as the mat only covers a fraction of the bonded surface. At intermediate adhesion levels, debonding and bridging will occur. However, as the mat covers only a small percentage of the polymer surface, there is only a small area that is capable of debonding, and hence the R-curve will be relatively limited.

6.2.2. Fibre-modified polymers

As stated above, not all of the fibre- and mat-modified resins gave an R-curve. The carbon short-fibres act more like a particulate modifier than a fibre modifier, as there was no apparent bridging across the fracture surfaces and, indeed, no R-curve was observed. The fracture surfaces revealed that the fibres were orientated approximately in the plane of the fracture, i.e. parallel to, and along the length of, the substrates, as may be expected due to the geometry of the TDCB specimen. However, fibre bridging and stretching was observed for the specimens made with the Kevlar short-fibres. The fibres were observed to bridge across the fracture surfaces, with debonding of the fibres occurring after fracture of the resin. This process of debonding and bridging causes the fracture energy to increase with increasing length of the propagating crack, and hence the presence of an R-curve was recorded. Thus, whilst the values of G_c at initiation for the carbon short-fibre and Kevlar short-fibre modified polymers are similar in value, the latter material shows a far greater maximum value of G_c at relatively high crack lengths, see Fig. 10. The PEEK fibres were also able to debond and bridge across the fracture surfaces, leading to a large R-curve, see Fig. 10. From the fractographic studies and the arguments developed in Fig. 18, it is suggested that the interfacial adhesion of the matrix to the carbon short-fibres is relatively good and this prevents debonding; which would, in turn, prevents the fibre pull-out and fibre-bridging mechanisms coming into play as the crack propagates. Hence, no R-curves are recorded for the carbon short-fibre modified polymers. On the other hand, the inferior adhesion which would be expected [2, 28] at the interfaces to the Kevlar and PEEK fibres would more readily allow the debonding and the subsequent bridging and toughening mechanism to occur, and hence enables R-curves to develop. As indeed is observed in Fig. 10. It appears that surface pre-treatment of the PEEK fibres, by using the plasma surface treatment, had no significant affect on these toughening mechanisms, see Fig. 10.

The fibre diameter may also have an effect on the toughening mechanisms. In addition to this process of debonding and bridging, relatively small diameter polymeric fibres which bridge across the fracture surfaces may exhibit considerable stretching. This will cause a further increase in the fracture energy as the crack propagates through the material. Hence, for the PEEK monofilaments, with a fibre diameter of approximately 200 μm, the stresses on the bridged monofilaments are insufficient to cause stretching and yielding of the fibres, and hence there is no additional energy absorption and no such toughening effect. However, the diameter of the PEEK fibres is much less and there is stretching and energy absorption by the fibres, again this is reflected in the data shown in Fig. 10. Monofilaments have been also used by Azam and Sargent [29] to toughen cyanate-ester polymers. However, in their work the PTFE monofilaments were laid across the

specimen, rather than along its length. In this case, a crack-pinning mechanism caused the toughening effect and, as expected, no R-curve was reported.

6.2.3. Woven-mat modified polymers

For the simple BADCy polymer, the specimens manufactured using the PEEK woven-mat showed a much smaller toughening effect compared to the use of the PEEK fibres, see Fig. 10. For example, the PEEK-fibre modified polymer showed, at 21°C, an R-curve that increased from 280 J/m^2 at short crack lengths to a maximum of 700 J/m^2. On the other hand, the R-curve for the PEEK woven-mat material increased from 135 J/m^2 to a maximum of 300 J/m^2. Indeed, compared to the simple, unmodified BADCy polymer, the addition of the woven-mat slightly reduced the fracture energy at short crack lengths. Hence, the adhesion between the PEEK mat and the polymer would be predicted to be relatively poor, in agreement with previous observations [22]. Indeed, failure did occur along one of the woven-mat/polymeric-matrix interfaces, as shown in Fig. 11; and very little bridging of the mat behind the advancing crack tip was observed. Hence, in agreement with the above arguments, the measured fracture energies were relatively low with no large R-curve being observed.

The Metlbond 2555G specimens provide a good example to demonstrate the effects of fibre bridging. At −55°C, a mean fracture energy of 210 J/m^2 was measured for initiation, with an R-curve increasing to a maximum of 290 J/m^2, see Fig. 14a. The locus of failure was mostly within the polymeric-matrix, although some fracture occurred at the interface of the glass woven-mat and the polymeric-matrix, see Fig. 19. Thus, it can be implied that the adhesion between the mat and the polymer is relatively strong. Indeed, inspection of the micrograph in Fig. 19b shows only a few areas where the fibres of the mat have debonded from the polymeric matrix on both sides, as indicated by the arrows. Furthermore, this debonding only occurs for a short distance before the fracture moves away from the interface and back into the polymeric matrix. As debonding only occurs in relatively small areas, rather than across the whole fracture surface, only a limited amount of bridging can occur. Hence the resulting R-curve for the Metlbond 2555G cyanate-ester material is relatively small.

For the Metlbond 2555G specimens tested at 21°C, a mean fracture energy of 150 J/m^2 was measured for initiation, with an R-curve increasing to 320 J/m^2 at a crack length of 190 mm, see Fig. 14b. The locus of failure was mostly along the glass woven-mat/polymeric-matrix interface, which debonded from the polymer and was observed to bridge across the fracture surfaces. However, some fracture occurred through the polymeric matrix, see Fig. 20. Inspection of the micrograph in Fig. 20b shows areas where the fibres of the mat have debonded from the polymeric matrix on both sides, as indicated by the arrows. These areas are now relatively large and more frequent than at −55°C, although this debonding still only occurs for a relatively short distance before the fracture moves away from the interface and back into the polymeric matrix. Thus, the R-curve for the Metlbond 2555G material is more pronounced at 21°C than at −55°C.

For the Metlbond 2555G specimens tested at 150°C, the fracture energy for the initiation of crack growth is somewhat increased, see Fig. 14c. The maximum value of the fracture energy also increased significantly with increasing temperature, from 290 J/m^2 at −55°C, to 450 J/m^2 at 150°C. Micrographs of the fracture surfaces showed that the locus of failure was along the mat/polymer interface at 150°C, with virtually no polymer being left on the fibres of the mat, compare Figs 19b, 20b and 21b. The woven-mat was also observed to debond from the polymeric matrix and bridge across the fracture surfaces during testing. Indeed, the glass woven-mat debonded from both of the fracture surfaces in many places, leading to a large amount of bridging. Fig. 21 shows micrographs of an area where debonding has occurred on both sides of the mat. It may be readily seen that the polymer has debonded from the top surface of the mat, shown in Fig. 21b, leaving an impression of the mat on the surface of the polymer, shown in Fig. 21a. In addition, in Fig. 21b, the polymer cannot be seen through the holes in the weave of the mat, indicating that it has also debonded from the bottom surface of the woven-mat. Hence the mat has debonded from both of the fracture surfaces, allowing significant bridging to occur which results in a very pronounced R-curve.

In the case of the BADCy polymers modified using the glass-fibre woven-mat carrier, then a similar picture to that for the Metlbond 2555G material may be deduced. However, micrographs of the fracture surfaces show that less polymer remains attached to the glass woven-mat for the mat-modified BADCy than for the Metlbond 2555G material, e.g. compare Figs 12 and 19. Hence, it appears that the interfacial adhesion between the BADCy polymer and the glass-mat is intermediate in nature. This, coupled with the observation that the woven-mat used in the mat-modified BADCy material covers a relatively large area, would lead from the above arguments to a far more pronounced 'R-curve' to be expected for the mat-modified BADCy polymers. This is indeed the experimental observation at all the test temperatures, as may be seen in Fig. 14a–c.

Finally, it should be noted that, the correlations between the type of physical modifier, the measured toughness, G_c, and the toughening mechanisms as deduced from the fractographic studies follow a similar pattern for the co-reacted phenol-BADCy polymers as for the simple BADCy polymers discussed in detail above.

6.3. Predictive modelling studies

The increases in the measured fracture energies due to the addition of the particulate-modifiers may be compared to the analytical model predictions from the theory developed by Faber and Evans [23]. These predictions describe the toughening effect caused by the deflection of the crack front when it reaches a particle. Faber and Evans modelled these predictions in the form of the relative fracture energy of the modified material (which is defined as the fracture energy of the

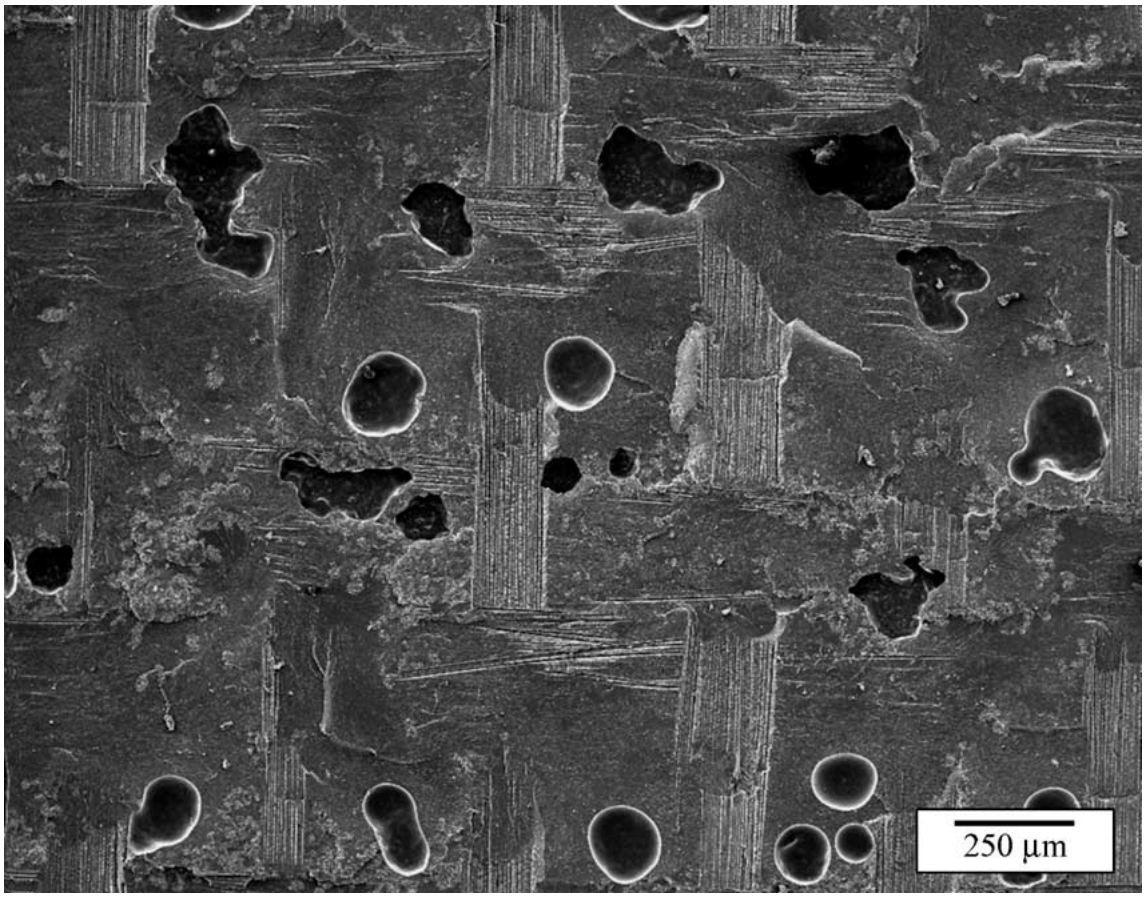

(a)

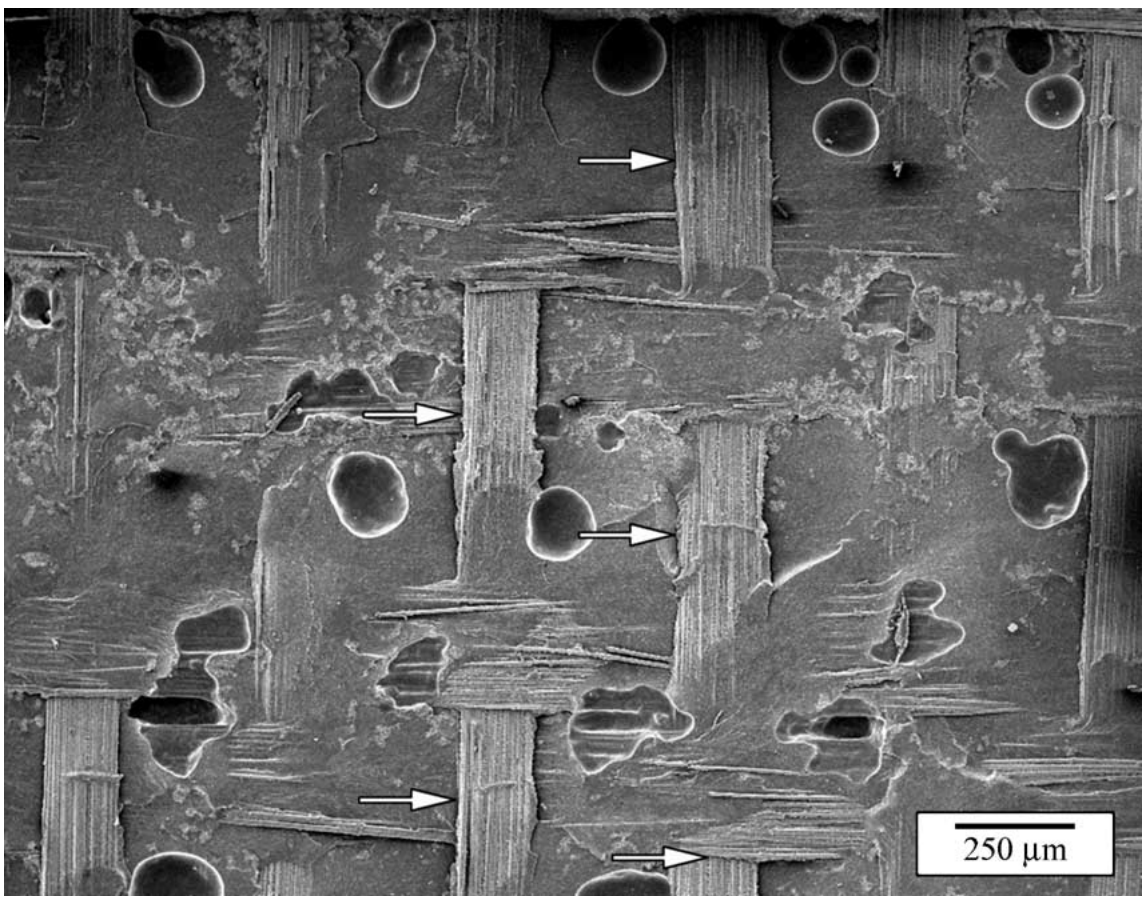

(b)

Figure 19 Fracture surfaces of the Metlbond 2555G tested at −55°C: (a) polymer side, and (b) mat side. The arrows indicate where the fibres of the mat have debonded from the polymeric matrix on both sides.

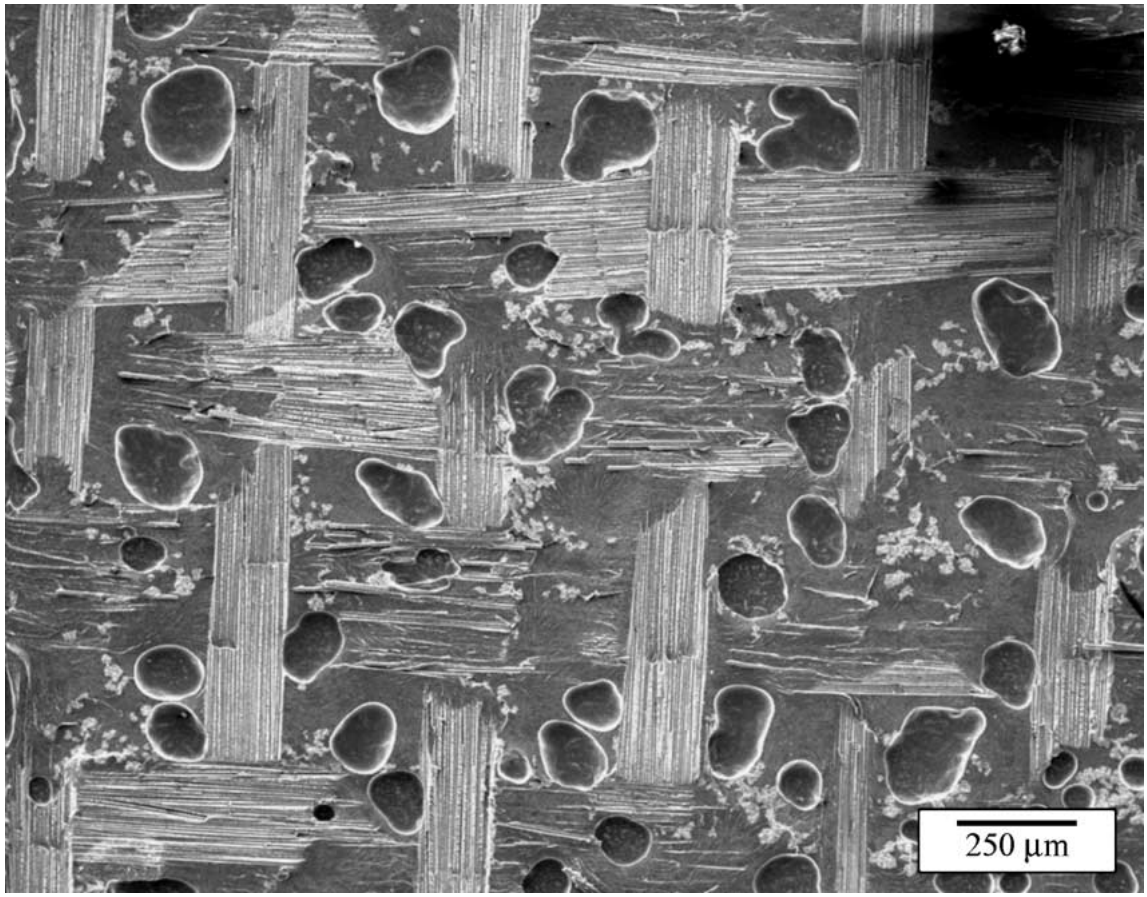

(a)

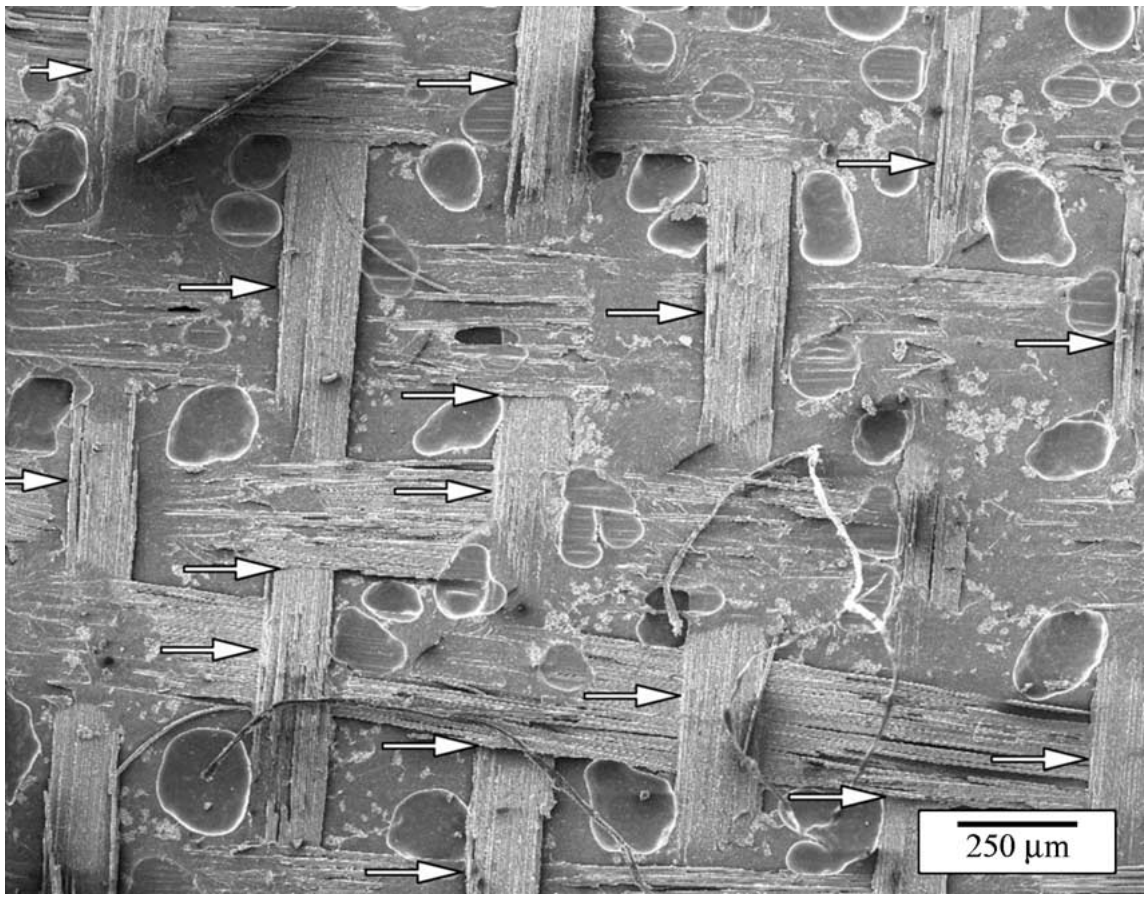

(b)

Figure 20 Fracture surfaces of the Metlbond 2555G tested at 21°C: (a) polymer side, and (b) mat side. The arrows indicate where the fibres of the mat have debonded from the polymeric matrix on both sides.

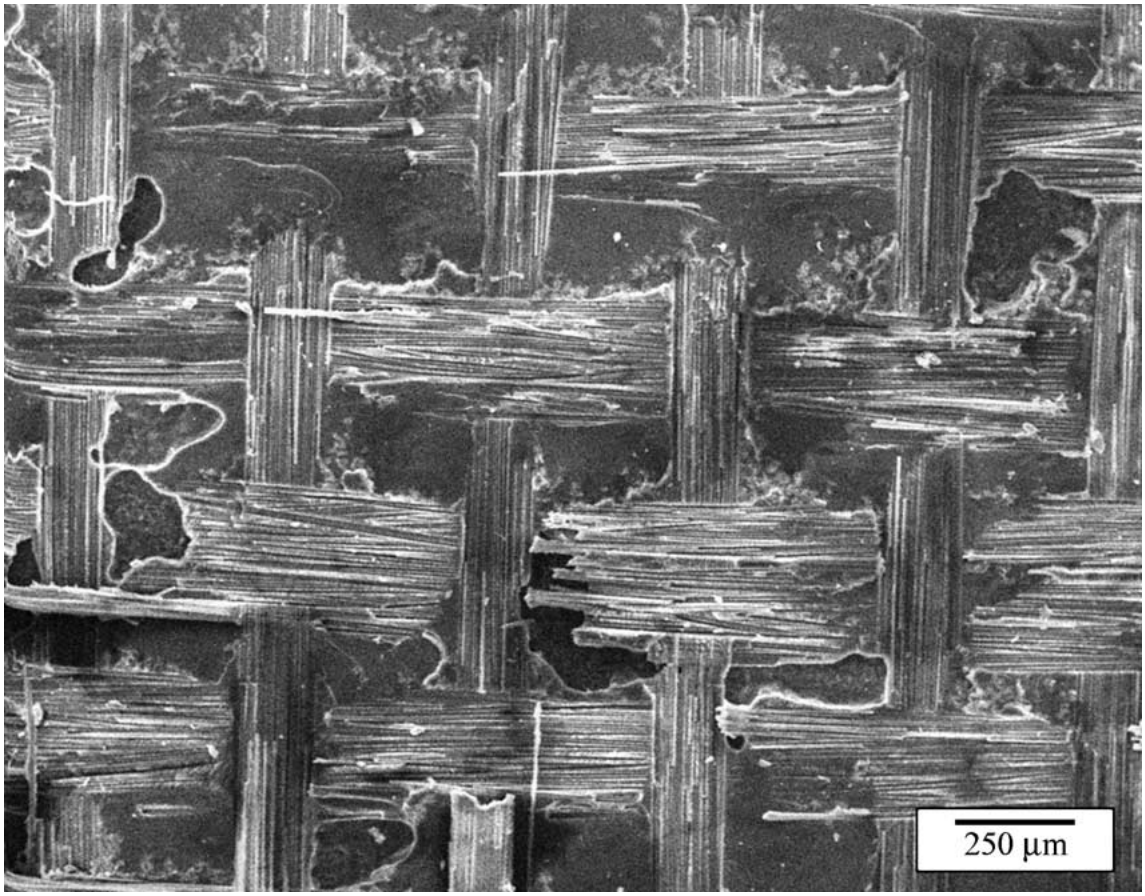

(a)

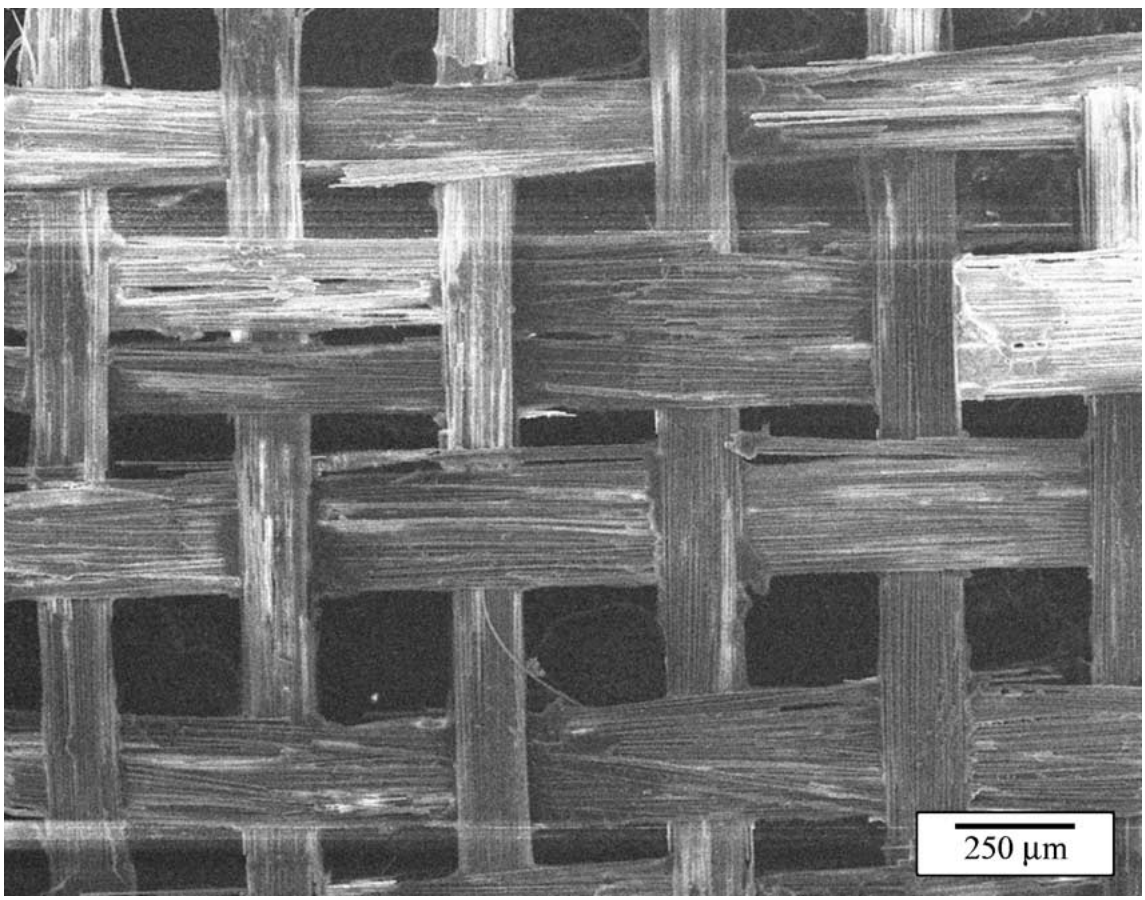

(b)

Figure 21 Fracture surfaces of the Metlbond 2555G tested at 150°C: (a) polymer side, and (b) mat side.

modified material normalised to that of the unmodified material) for sphere-, rod- and plate-shaped particles, as a function of the volume fraction and aspect ratio of the physical modifier.

The Faber and Evans analysis [23] uses a crack deflection model. When an advancing crack encounters a particle, there is an initial deflection of the crack which tilts the crack out of its advancing plane. Subsequent twisting and tilting of the crack occurs as the deflected crack encounters further particles. The increased area of the fracture surface causes a small increase in the measured fracture toughness. However, the deflected crack is now subjected to mixed-mode loading. The tilted crack experiences mode I (tensile) and mode II (in-plane shear) loading, while the twisted crack experiences mode I and mode III (anti-plane shear) loading. It is well-known that fracture under mode II and mode III loading requires more energy than in mode I, and hence the local mode-mix increases the measured fracture energy in a nominally mode I fracture test.

The volume fraction of the modifier can be calculated from the weight fraction using the densities of the modifier and resin. For example, the density of the simple BADCy resin is 1.26 g/cm^3 [30, 31], and that of the hollow glass spheres is 1.10 g/cm^3 [32]. As noted above, the relative fracture energy is calculated by dividing the measured fracture energy of the modified BADCy polymer by that of the unmodified BADCy polymer. Hence, from the present experimental studies, the addition of hollow glass spheres, at 10 or 20% by weight, to the simple BADCy polymer gives relative fracture energies of between 1.2 and 1.8 as the test temperature is varied from −55 to 150°C. These values agree well with the predictions obtained from Fig. 6 of the Faber and Evans paper [23], as shown in Table III. The best agreement is obtained by assuming a uniform spacing of spheres in the resin, rather than a distributed spacing, although the experimental value at 150°C is slightly higher than predicted, see Table III.

A similar analysis can be performed for the rod-like wollastonite and carbon short-fibre physical modifiers.

TABLE III Predicted and experimental relative fracture energies for the simple BADCy polymer modified with the hollow glass spheres

		Relative fracture energy				
		Prediction		Experimental		
Weight fraction	Volume fraction	Uniform spacing	Distributed spacing	−55°C	21°C	150°C
0.1	0.11	1.27	1.48	1.22	1.25	1.81
0.2	0.23	1.32	1.63	–	1.33	–

When aspect ratios of 3 or 12 are used, the predicted data may be directly read off Fig. 13 of the Faber and Evans paper [23]. These predicted relative fracture energies are compared to the experimental values in Table IV. The true aspect ratio of the wollastonite particles is approximately four, as they are about 60 μm long by 15 μm in diameter, so the experimental relative fracture energies should lie between the tabulated values. However, the experimental values are much smaller than the predicted values. The mean aspect ratio of the carbon short-fibres is about 140, the fibres being 1 mm long and 7 μm in diameter. As the relative fracture energy increases with aspect ratio, the experimental value should be higher than the predicted values shown in the Table IV. However, the experimental value is actually lower than the predicted value for an aspect ratio of 3. Indeed, this experimental value is approximately equal to the prediction for an equivalent volume fraction of spheres. Hence the rod-like shape of the wollastonite particles does not increase the fracture energy to the extent predicted by Faber and Evans.

Disc-like mica particles were also used in the present work. The relative fracture energies were again predicted using the analysis of Faber and Evans, and compared to the experimental data. Three grades of mica were used, with mean particle diameters of 80 μm, 40 μm and 10 μm. The particles have a mean thickness of about 5 μm. This gives aspect ratios of 16, 8 and 2 respectively for the mica particles of the different mean particle sizes. The agreement between the experimental and predicted values was relatively good for the smallest particle size material, the measured values lying within about 10% of the predicted fracture energies. However, as the particle size and aspect ratio of the mica particles increased, then the agreement between the experimental and predicted values become poorer. For the largest mica particles used, the experimental values were about 40% lower than the predicted values.

Thus, although agreement between the predictions and the experimental data is good for the spherical and the small disc-shaped particles of the hollow glass and the 10 μm mica modifiers respectively, it is relatively poor for the rods and large disc-shaped particles. However, as noted above, scanning electron microscopy studies of the fracture surfaces showed that the larger mica flakes, for example, tend to lie relatively flat on the surface. This is due to the spreading action used to coat the substrate with the modified-BADCy resin. Hence, the angle of the flakes relative to the direction of crack propagation is not random, as the predictive model of Faber and Evans assumes. This will reduce

TABLE IV Predicted and experimental relative fracture energies for the simple BADCy polymer modified with the rod-like wollastonite particles and the carbon short-fibres

			Relative fracture energy				
			Prediction		Experimental		
Modifier	Weight fraction	Volume fraction	Aspect ratio = 3	Aspect ratio = 12	−55°C	21°C	150°C
Wollastonite	0.1	0.15	2.24	3.85	0.93	1.15	2.00
Carbon fibre	0.1	0.07	1.97	3.70	–	1.29	–

the amount of tilt and twist of the crack front, and hence the fracture energy will be lower than for a truly random, isotropic particulate-modified material. The anisotropy of the orientation of the particles will be more accentuated for larger particles, and hence the rate of increase of the fracture energy will reduce as the particle size is increased. As expected from this argument, this is especially the case for the carbon short-fibres, which are much longer than the thickness of the layer of polymer in the TDCB specimens.

7. Conclusions

A fracture mechanics approach has been used to investigate the effect of the addition of physical modifiers on the toughness of a high-temperature, but basically brittle, cyanate-ester polymer. Tests were performed using tapered-double cantilever-beam (TDCB) adhesive joint specimens at −55, 21 and 150°C. A range of inorganic and organic particles, fibres and woven-mats have been used in an attempt to enhance the fracture properties of simple and phenol co-reacted modified cyanate-ester, termed 'BADCy', polymers. The glass transition temperature, T_g, of the simple BADCy polymer was 310°C and that of the 10% phenol-BADCy polymer was 228°C. This reduction of the T_g is due the co-reaction of the mono-functional phenol into the polymer network. The fracture energies, G_c, of these materials have been measured and scanning electron microscopy has been used to determine the toughening micromechanisms involved.

Considering the particles and fibres, then the most successful inorganic modifier was mica which at the optimum concentration of 10% by weight gave a fracture energy of 302 J/m^2 at 21°C, compared to 150 J/m^2 for the unmodified simple BADCy polymer. This value of G_c was not greatly affected by the test temperature. For example, a value of 248 J/m^2 was recorded at 150°C, which is a major increase compared to the value of 90 J/m^2 for the unmodified BADCy polymer at this temperature. There was no significant effect of the particle size of the mica upon going from a mean particle size of 10 μm to 80 μm. The inclusion of nanometre-sized particles all tended to reduce the measured fracture energy compared to that of the unmodified BADCy polymer, probably due to severe aggregation of the nano-particles. Considering the organic-particulate modifiers, the addition of PTFE particles resulted in a large increase in the measured fracture energy at 150°C due to softening of the PTFE. The addition of 10% of PEEK particles to the unmodified BADCy resin also gave a significant increase in the fracture energy to about 250 J/m^2. This value was relatively insensitive to the test temperature, as would be expected since PEEK softens less than PTFE at 150°C. The main toughening micromechanisms which were identified as being operative for these materials were a combination of (a) crack pinning and deflection and (b) plastic hole growth around the particles. Comparison of the experimental results to the values predicted, using a previous analytical model for such materials from the work of Faber and Evans [23], showed good agreement for low aspect-ratio particles. The Faber and Evans' model assumes a random, isotropic material, as observed for these low aspect-ratio systems. However, as the aspect ratio was increased, fractography showed that the orientation of the particles became anisotropic, hence the agreement between the experimental and predicted values became relatively poor.

The use of long fibres or woven-mats as physical modifiers for the polymers gave an increase of the fracture energy at initiation and also gave a further increase in the fracture energy as the crack propagated through the specimen; i.e. an R-curve was observed. For example, the fracture energy of the simple BADCy polymer was increased from 150 to 230 J/m^2 at crack initiation using a woven glass-mat, but then increased to 940 J/m^2 at long crack lengths, i.e. as the R-curve developed. For the fibre- and woven-mat modified polymers, a significant increase in the fracture energy with crack length was observed when there was significant fibre bridging across the fracture surfaces. Indeed, bridging of the fibres, or the woven-mat, across the fracture surfaces behind the advancing crack tip was identified as the major toughening micromechanism and the main cause of the observed R-curve. A commercially-available cyanate-ester film-adhesive (Metlbond 2555G; $T_g = 232$°C), which contained a glass woven-mat carrier, was also evaluated.

Finally, it is noteworthy that the toughest of the materials developed in the present study was the co-reacted 10% phenol-BADCy polymer which was physically modified using the glass-fibre woven-mat. For example, at 21°C, this material possessed a mean initial G_c value of 544 J/m^2 and this rose to over 1000 J/m^2 for the steady-state crack propagation value of G_c. This compares to values of about 175 J/m^2 and 300 J/m^2 respectively at 21°C for the commercial Metlbond 2555G adhesive; and to 220 J/m^2 for the unmodified 10% phenol-BADCy polymer and 150 J/m^2 for the unmodified simple BADCy polymer. Further, the values for the woven-mat modified 10% phenol-BADCy polymer quoted above were not significantly decreased when the tests were conducted at 150°C. The values of the woven-mat modified simple BADCy polymer, which had a T_g some 80°C higher, were of a similar order but were significantly lower at all the test temperatures.

Acknowledgements

The authors would like to thank Isola AG (Düren, Germany) for supplying the resin monomer, and Dr. Christoph Uhlig at the Institüt Fraunhofer Zuverlässigkeit und Microintegration for prepolymerising the resin and formulating the phenol blends. We would also like to thank Dr. Jeff Sargent at BAe Systems, Microfine Minerals and Potters-Ballotini for supplying samples of fibre, mat and particulate toughners. We would like to thank the European Commission for their financial support of this work (BE96-3947/BRPR-CT97-0418). Ambrose Taylor is a Royal Academy of Engineering Post-Doctoral Research Fellow, and would like to thank the Royal Academy of Engineering for their support.

References

1. B. HUSSEY and J. WILSON, "Structural Adhesives: Directory and Databook" (Chapman & Hall, London, 1996).
2. A. J. KINLOCH, "Adhesion and Adhesives: Science and Technology" (Chapman Hall, London, 1987).
3. A. W. SNOW, in "Chemistry and Technology of Cyanate Ester Resins," edited by I. Hamerton (Blackie Academic & Professional, Glasgow, 1994) p. 7.
4. R. B. GRAVER, in "International Encyclopaedia of Composites," edited by S. M. Lee (VCH Publishers, Cambridge, 1990) Vol. 1, p. 549.
5. D. A. SHIMP, in "Chemistry and Technology of Cyanate Ester Resins," edited by I. Hamerton (Blackie Academic & Professional, Glasgow, 1994) p. 282.
6. I. HAMERTON, in "Chemistry and Technology of Cyanate Ester Resins," edited by I. Hamerton (Blackie Academic & Professional, Glasgow, 1994) p. 1.
7. M. BAUER and J. BAUER, in "Chemistry and Technology of Cyanate Ester Resins," edited by I. Hamerton (Blackie Academic & Professional, Glasgow, 1994) p. 58.
8. A. J. KINLOCH and A. C. TAYLOR, to be published.
9. British Standards Institute, BS-EN-573-1 (BSI, London, 1994).
10. C. UHLIG, Personal Communication, Fraunhofer Institüt Zuverlässigheit und Microintegration, 1997.
11. UK Defence Standard 03-2/2 (1983).
12. "Adhesion, Adhesives and Composites Website, http://www.me.ic.ac.uk/materials/AACgroup/index.html" (Imperial College of Science, Technology and Medicine, 2001).
13. B. R. K. BLACKMAN and A. J. KINLOCH, in "Fracture Mechanics Testing Methods for Polymers, Adhesives and Composites," edited by A. Pavan, D. R. Moore and J. G. Williams (Elsevier Science, Amsterdam, 2001) p. 225.
14. B. R. K. BLACKMAN, A. J. KINLOCH, A. C. TAYLOR and Y. WANG, *J. Mater. Sci* **35** (2000) 1867.
15. B. R. K. BLACKMAN, J. P. DEAR, A. J. KINLOCH, H. MACGILLIVRAY, Y. WANG, J. G. WILLIAMS and P. YAYLA, *ibid.* **30** (1995) 5885.
16. S. MOSTOVOY and E. J. RIPLING, *J. Appl. Polymer Sci.* **10** (1966) 1351.
17. D. A. SHIMP and S. J. ISING, in Proceedings of the 35th International SAMPE Symposium and Exhibition, Anaheim, CA, USA (SAMPE, Covina, CA, USA, 1990).
18. E. H. ANDREWS, "Fracture in Polymers" (Oliver & Boyd, Edinburgh, 1968).
19. R. E. GRIM, "Applied Clay Mineralogy" (McGraw-Hill, New York, 1962).
20. Microfine-Minerals, "Datasheet."
21. P. BEGUELIN and H. H. KAUSCH, *J. Mater. Sci.* **29** (1994) 91.
22. B. R. K. BLACKMAN, A. J. KINLOCH and J. F. WATTS, *Composites* **25** (1994) 332.
23. K. T. FABER and A. G. EVANS, *Acta Metal.* **31** (1983) 565.
24. *Idem.*, *ibid.* **31** (1983) 577.
25. A. J. KINLOCH, D. L. MAXWELL and R. J. YOUNG, *J. Mater. Sci. Lett.* **4** (1985) 1276.
26. *Idem.*, *J. Mater. Sci.* **20** (1985) 4169.
27. Goodfellow Ltd., "Catalogue" (1998).
28. A. J. KINLOCH, G. K. A. and J. F. WATTS, *Phil. Trans. R. Soc. Lond.* **A338** (1992) 83.
29. S. AZAM and J. P. SARGENT, *J. Adhesion* **71** (1999) 1.
30. Z. CAO, F. MECHIN and J. PASCAULT, *Polymer Int.* **34** (1994) 41.
31. I. HAMERTON, in "Chemistry and Technology of Cyanate Ester Resins," edited by I. Hamerton (Blackie Academic & Professional, Glasgow, 1994) p. 329.
32. Potters-Ballotini, "Sphericel Datasheet."

Received 1 June
and accepted 23 July 2001